RIFT-BASIN STRUCTURE AND ITS INFLUENCE ON SEDIMENTARY SYSTEMS

MARTHA OLIVER WITHJACK AND ROY W. SCHLISCHE

Department of Geological Sciences, Rutgers University, Piscataway, New Jersey 08854-8066, U.S.A.
e-mail: drmeow3@rci.rutgers.edu; schlisch@rci.rutgers.edu

AND

PAUL E. OLSEN

Lamont-Doherty Earth Observatory of Columbia University, Palisades, New York 10964, U.S.A.
e-mail: polsen@ldeo.columbia.edu

ABSTRACT: Rift basins are complex features defined by several large-scale structural components including faulted margins, the border faults of the faulted margins, the uplifted flanks of the faulted margins, hinged margins, deep troughs, surrounding platforms, and large-scale transfer zones. Moderate- to small-scale structures also develop within rift basins. These include: basement-involved and detached normal faults; strike-slip and reverse faults; and extensional fault-displacement, fault-propagation, forced, and fault-bend folds.

Four factors strongly influence the structural styles of rift basins: the mechanical behavior of the prerift and synrift packages, the tectonic activity before rifting, the obliquity of rifting, and the tectonic activity after rifting. On the basis of these factors, we have defined a standard rift basin and four end-member variations. Most rift basins have attributes of the standard rift basin and/or one or more of the end-member variations. The standard rift basin is characterized by moderately to steeply dipping basement-involved normal faults that strike roughly perpendicular to the direction of maximum extension. Type 1 rift basins, with salt or thick shale in the prerift and/or synrift packages, are characterized by extensional forced folds above basement-involved normal faults and detached normal faults with associated fault-bend folds. In Type 2 rift basins, contractional activity before rifting produced low-angle thrust faults in the prerift strata and/or crystalline basement. The reactivation of these contractional structures during rifting created the low-angle normal faults characteristic of Type 2 rift basins. In Type 3 rift basins, preexisting zones of weakness in the prerift strata and/or crystalline basement strike obliquely to the direction of maximum extension, leading to oblique rifting. Type 3 rift basins are characterized by faults with strike-slip, normal, and oblique-slip displacement and with multiple trends. Contractional activity followed rifting in Type 4 rift basins. These inverted rift basins are affected by late-formed contractional structures including normal faults reactivated with reverse displacement, newly formed reverse faults, and contractional fault-bend and fault-propagation folds.

Structures within rift basins affect depositional patterns by creating sites of uplift and erosion, by controlling pathways of sediment transport, and by defining the accommodation space for sediment deposition and preservation. The relationships among basin capacity (structurally controlled), sediment supply, and water supply determine the primary depositional regime in nonmarine rift basins, fluvial or lacustrine. Changes in basin capacity resulting from the growth of a rift basin may yield a tripartite stratigraphy (fluvial, deep lacustrine, and shallow lacustrine–fluvial) common to many nonmarine rift basins.

INTRODUCTION

Knowledge of continental rifting has increased steadily during the past several decades. Field geologists have more precisely defined the timing and style of deformation in many exposed rift basins (e.g., the Newark basin of eastern North America, the Upper Rhine rift basin of central Europe, and Kenya basin of East Africa). Simultaneously, seismic interpreters, using 2D and 3D data acquired during hydrocarbon exploration and production activities, have identified and mapped many of the world's subsurface rift basins (e.g., the Viking and Central rift basins of the North Sea, the Jeanne d'Arc rift basin of the Canadian Grand Banks, and the Dampier rift basin on the Northwest Shelf of Australia). Additionally, experimentalists have used scaled laboratory models to simulate rift-basin development under a variety of geologic conditions. Together, these field, seismic, and experimental approaches have yielded valuable information about the structural styles and depositional patterns of rift basins.

Most previous reviews of rift-basin structures have focused on one particular rift system using one, or possibly two, of the above approaches (e.g., Rosendahl, 1987; Schlische, 1993; Morley, 1995, 1999b). In this paper, we examine rift systems from around the world, using information provided by field, seismic, and experimental approaches. This broad perspective allows us to describe the variety of structures associated with continental rifting and to infer the influence of these structural styles on the depositional patterns within them. Because of space limitations,

we have left out or abbreviated many important topics related to continental rifting. Readers interested in tectonic-scale aspects of rifting and continental extension should consult the review papers by Roberts and Yielding (1994), Leeder (1995), and Ruppel (1995). Also, Peacock et al. (2000) presented a useful compilation of the voluminous nomenclature related to normal faults, rift basins, and extensional tectonics.

RIFT BASINS AND RIFT SYSTEMS

Rift basins are elongate crustal depressions bounded on one or both sides by basement-involved normal faults (i.e., faults that cut the crystalline basement) (Figs. 1 and 2). These extensional features are up to several kilometers deep, tens of kilometers wide, and hundreds of kilometers long. Rift systems are collections of stepping, intersecting, and/or parallel rift basins (e.g., Nelson et al., 1992) (Fig. 3). For example, the Bresse and Upper Rhine rift basins of southern France and Germany are right-stepping rift basins that form part of the Tertiary rift system of central Europe (e.g., Ziegler, 1992) (Fig. 3B). The Culpeper and Taylorsville rift basins of the southeastern United States are parallel rift basins that form part of the Mesozoic rift system of eastern North America (e.g., Withjack et al., 1998) (Fig. 3C). Although many rift systems are associated with continental breakup and passive-margin development (e.g., the Mesozoic rift system of eastern North America), rift systems can form in a variety of tectonic settings. For example, the Tertiary rift system
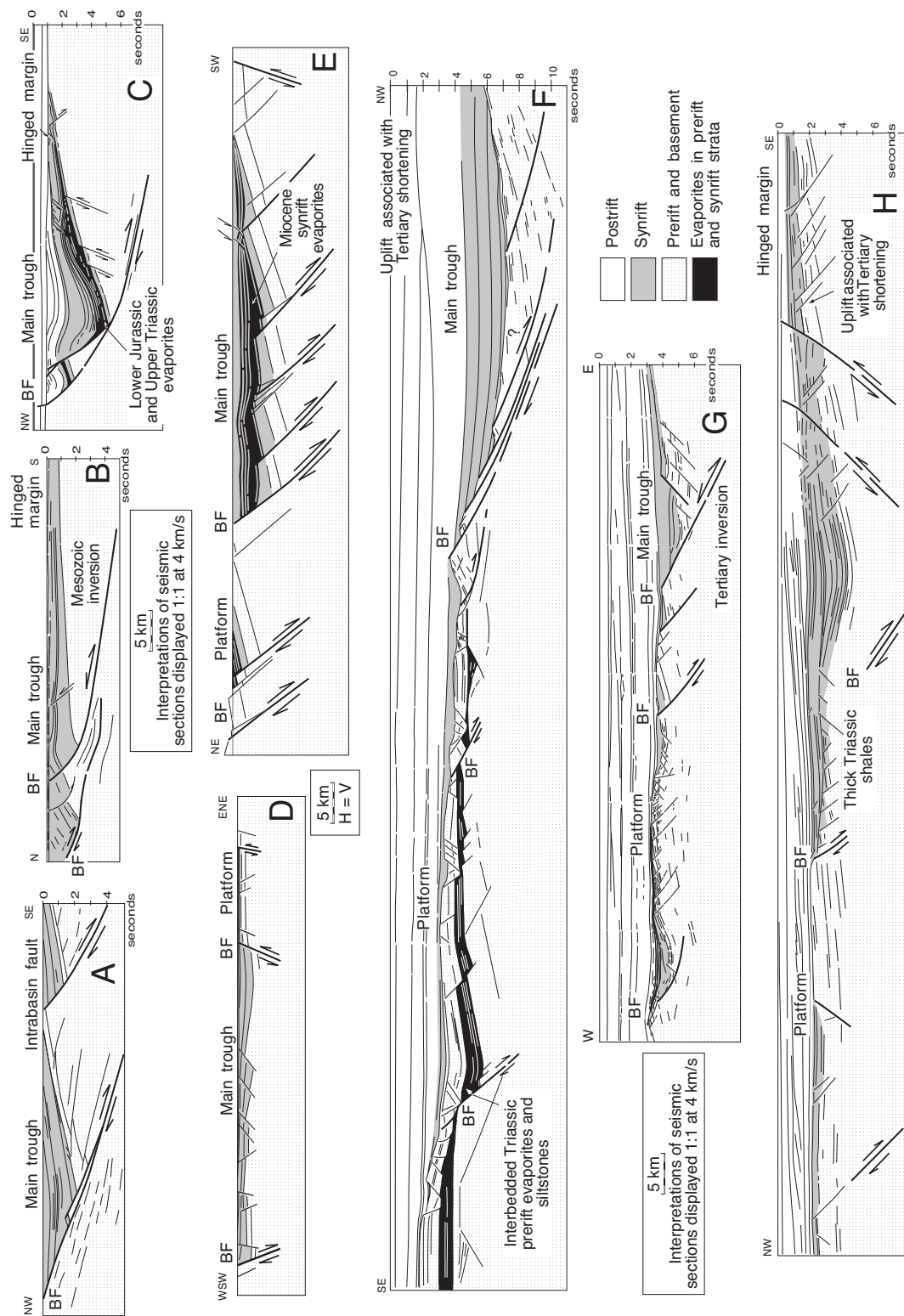
FIG. 1—Cross sections of rift basins. All of the sections have the same horizontal scale, and are shown with the faulted margin and border faults (BF) on the left. The geologic cross sections are displayed without vertical exaggeration. The seismic sections are displayed without vertical exaggeration assuming a velocity of 4 km / s; the vertical axes are in seconds of two-way travel time. **A)** Line drawing of seismic line NB-1 through the Mesozoic Newark rift basin, eastern United States (after Withjack et al., 1998). Figure 2A gives the line location. **B)** Line drawing of seismic line 81–47 through the Mesozoic Fundy rift basin, southeastern Canada (after Withjack et al., 1998). **C)** Line drawing of seismic line 85–4A through the Mesozoic Jeanne d' Arc rift basin, southeastern Canada (after Withjack and Callaway, 2000). **D)** Geologic cross section through the Tertiary Upper Rhine rift basin, Germany (after Sittler, 1969). Figure 2B gives the section location. **E)** Geologic cross section through the Tertiary Suez rift basin, Egypt (after Colletta et al., 1988). Figure 2C give the section location. **F)** Line drawing of a segment of seismic line GMNR94-310 through the Mesozoic Vøring rift basin of offshore Norway (after Withjack and Ingebrigtsen, 1999; Withjack and Callaway, 2000). **G)** Composite line drawing of several seismic lines through the Mesozoic Viking rift basin, northern North Sea. **H)** Composite line drawing of several seismic lines through the Mesozoic Dampier rift basin of the Northwest Shelf, offshore Australia (after Withjack and Eisenstadt, 1999; Schlische et al., 2002). Figure 2D gives the line location.
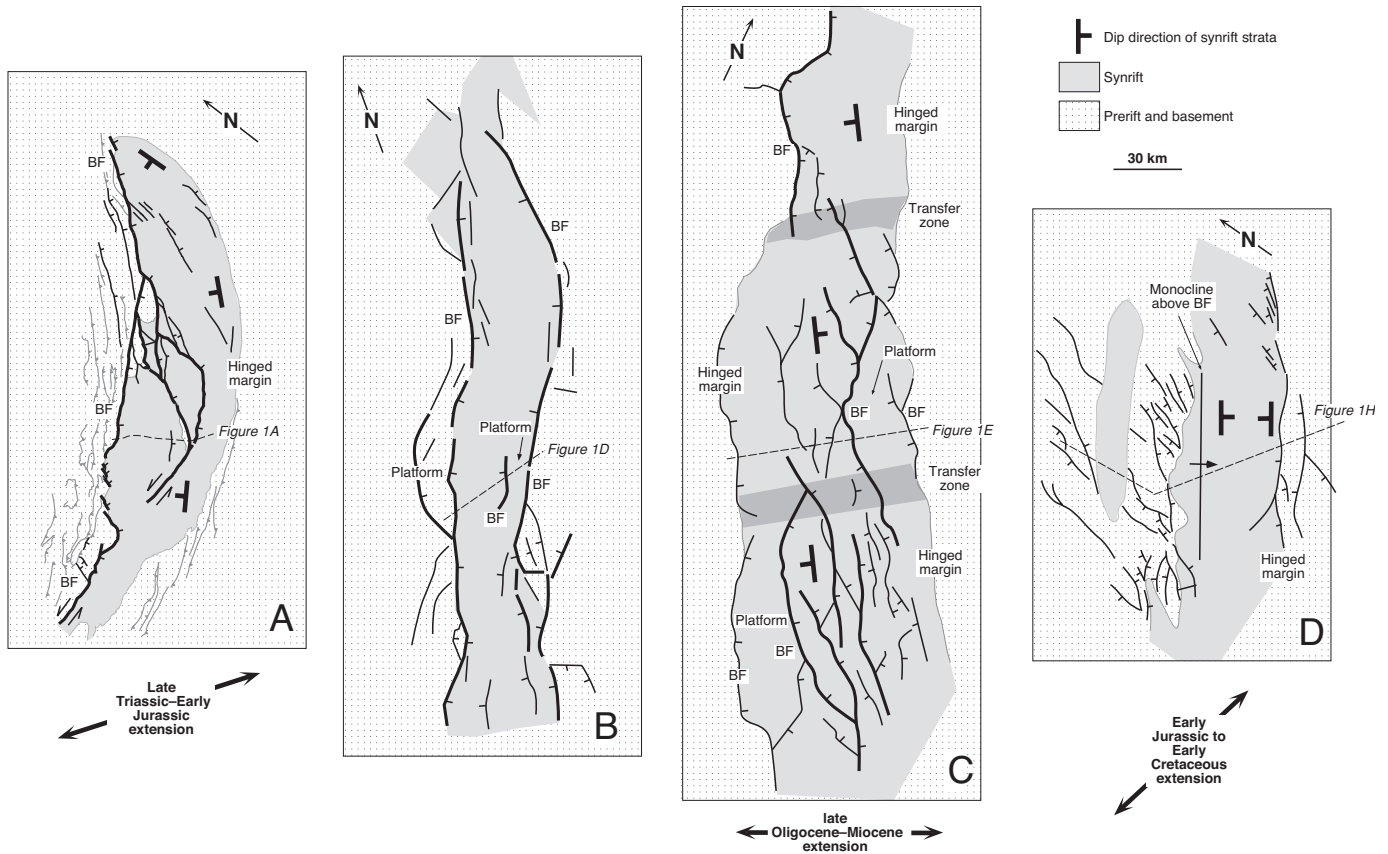
FIG. 2.—Map views of rift basins. All maps are shown at the same scale, and are oriented such that the rift axis is vertical. Thin black lines are normal faults with more than several hundred meters of displacement. Thick black lines are normal faults with several kilometers of displacement. BF is border fault. **A)** Mesozoic Newark rift basin, eastern United States (after Schlische, 1992). The strike of the rift-basin border faults is subparallel to the strike of the Paleozoic reverse faults (gray barbed lines). **B)** Tertiary Upper Rhine rift basin, Germany (after Breyer, 1974; Illies and Greiner, 1978). **C)** Tertiary Suez rift basin, Egypt (after Patton et al., 1994). **D)** Mesozoic Dampier rift basin of Northwest shelf, offshore Australia (after Withjack and Eisenstadt, 1999; Schlische et al., 2002). The strike of many of the normal faults on the northwestern margin of the basin is oblique to the trend of the rift axis.

of central Europe developed adjacent to the active Alpine collision zone (e.g., Ziegler, 1992) (Fig. 3B), whereas the Mesozoic rift system of eastern North America formed within a Paleozoic orogenic belt (e.g., Withjack et al., 1998) (Fig. 3C).

LARGE-SCALE STRUCTURAL COMPONENTS OF RIFT BASINS

Rift basins are complex features defined by several large-scale structural components. These components include faulted margins, the border faults of the faulted margins, the uplifted flanks of the faulted margins, hinged margins, deep troughs, large-scale intrabasin fault blocks, and large-scale transfer zones (Figs. 1 and 2).

Faulted Margins

Basement-involved normal faults with displacements of several kilometers and lengths of several tens of kilometers are a fundamental part of every faulted margin. These faults are commonly called border faults, and their spatial arrangement varies considerably (Fig. 4). Some border faults have a stepping geom-

etry and similar dip directions, forming asymmetric rift basins with a faulted margin and a hinged margin (Fig. 4A). For example, the northwestern faulted margin of the asymmetric Newark rift basin is composed of closely spaced, right-stepping, southeast-dipping, basement-involved normal faults (e.g., Withjack et al., 1998) (Figs. 1A and 2A). Some border faults have a stepping geometry and convergent dip directions, causing the faulted and hinged margins to shift from side to side of the rift basin (Fig. 4B). For example, the faulted and hinged margins shift from side to side in the Suez rift basin (e.g., Moustafa, 1976; Thiebaud and Robson, 1979; Colletta et al., 1988) (Fig. 2C) and in many of the rift basins of the East African rift system (e.g., Rosendahl et al., 1986; Ebinger et al., 1987; Morley et al., 1990). Some border faults are parallel, overlapping, and have similar dip directions (Fig. 4C). The fault blocks between these border faults are called platform structures in the Upper Rhine rift basin (Breyer, 1974) (Figs. 1D and 2B), stepfault platforms in the Kenya rift basin (Baker and Wohlenberg, 1971), border zones in the Suez rift basin (Garfunkel and Bartov, 1977) (Figs. 1E and 2C), benches in the Rio Grande rift basin (Kelley, 1979), and terraces in the Vøring rift basin of offshore Norway (Blystad et al., 1995) (Fig. 1F). Some border faults are parallel, overlapping, and have con-
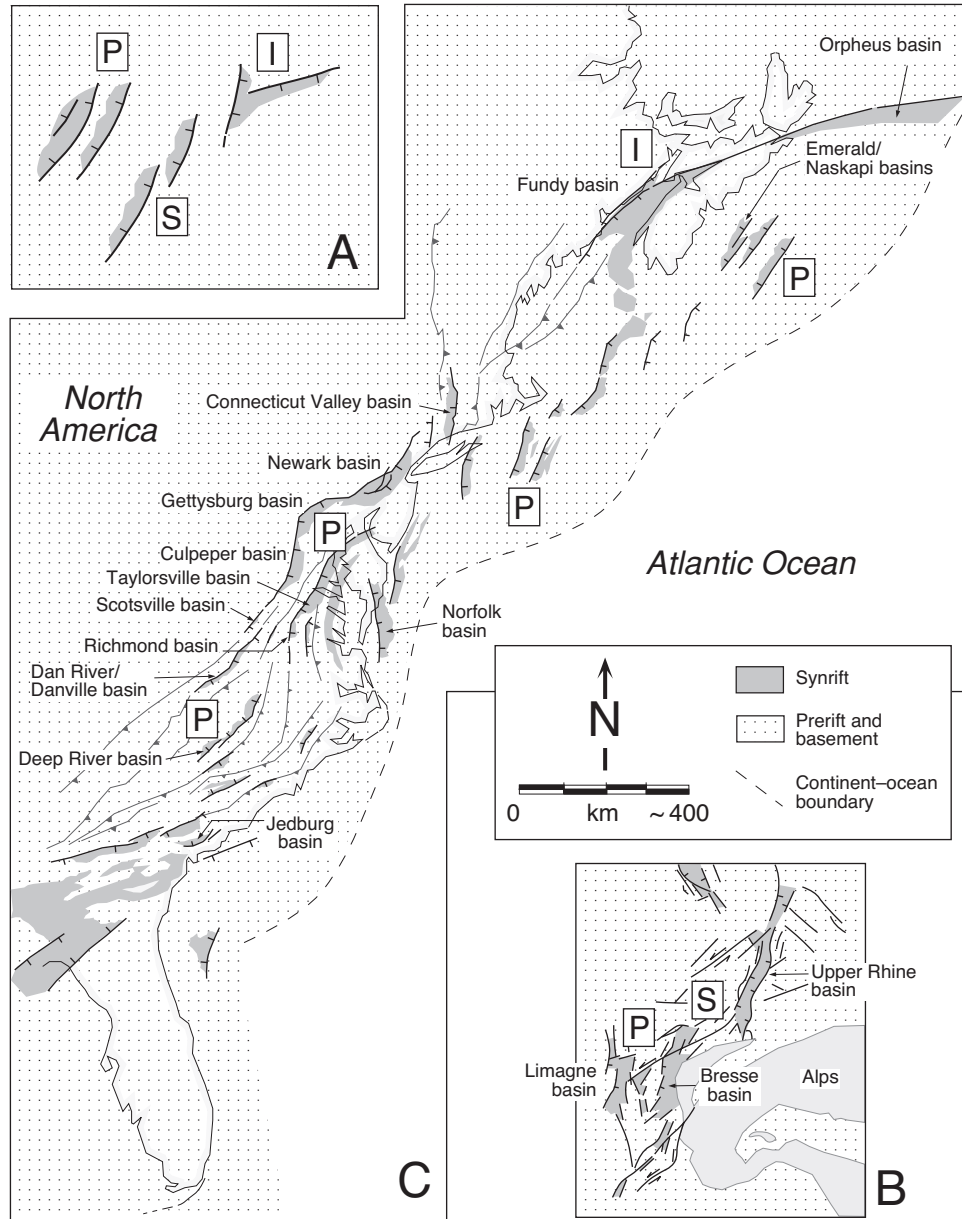
FIG. 3.—Map views of rift systems. Maps B and C are shown at the same scale. **A)** Schematic drawing of parallel (P), stepping (S), and intersecting (I) rift basins. **B)** Tertiary rift system of central Europe, showing a right-stepping arrangement of the Upper Rhine and Bresse rift basins and a parallel arrangement of the Bresse and Ligmagne rift basins (after Ziegler, 1992). Note the proximity of the coeval Alpine collision zone. **C)** Mesozoic rift system of eastern North America, showing parallel and intersecting rift basins (after Withjack et al., 1998). The rift system is now part of the Atlantic passive margin. It formed within a Paleozoic orogenic belt. The strike of the rift-basin border faults is subparallel to the strike of the Paleozoic contractional structures (gray, barbed lines).

vergent dip directions, forming symmetric rift basins with two faulted margins and no hinged margin (Fig. 4D). For example, the western and eastern faulted margins of the symmetric Upper Rhine rift basin are composed of east- and west-dipping border faults, respectively (e.g., Sittler, 1969) (Figs. 1D and 2B). Finally, some border faults intersect each other (Fig. 4E). For example, the northwestern faulted margins of the Fundy and Chignecto rift basins are composed of northeast-striking, basement-involved normal faults. An intersecting east-striking, basement-involved fault with both normal and strike-slip components of displace-

ment bounds the adjoining Minas rift basin (Withjack et al., 1995b) (see Figs. 7C and 7D).

The secondary deformation associated with border faults also varies considerably. In many rift basins, folds form in the sedimentary cover above the border faults. For example, monoclinal flexures occur above the border faults of the southern Upper Rhine rift basin (Laubscher, 1982; Maurin, 1995) (see Fig. 12E) and in the Haltenbanken area of offshore Norway (Fig. 1F). Evaporites in the prerift package facilitated the development of these folds by decoupling the shallow strata from the deep,
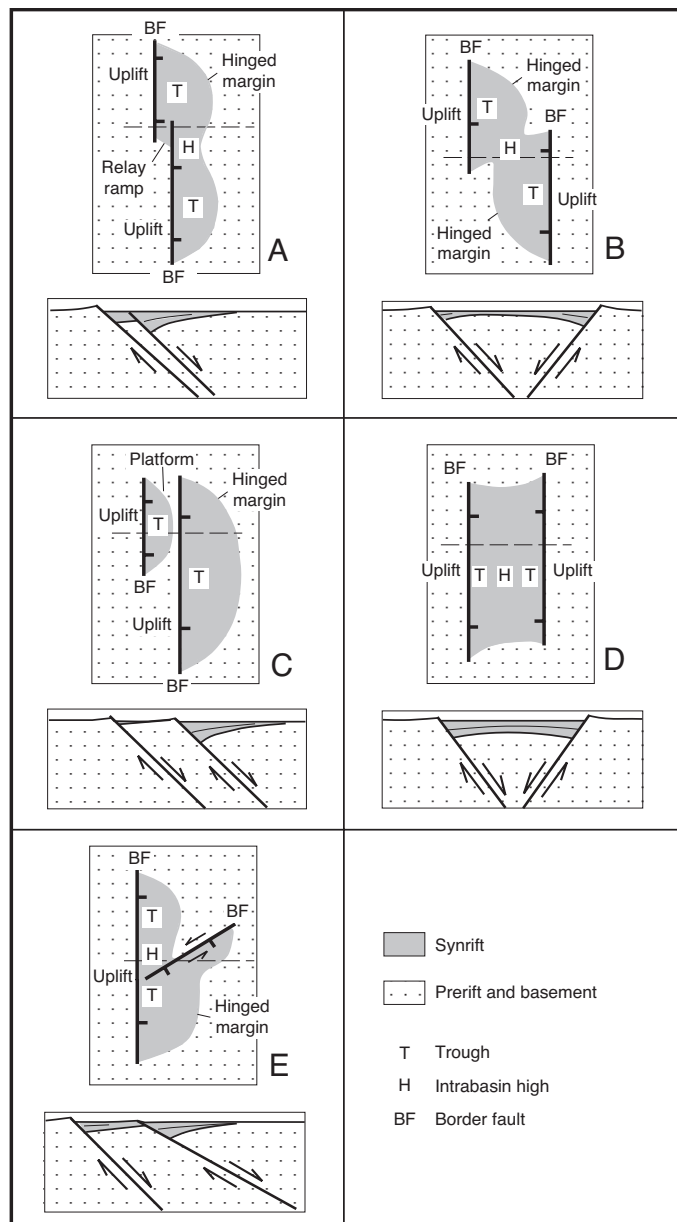
FIG. 4.—Arrangement of rift-basin border faults. The maps are displayed at half the size of the cross sections. **A)** Border faults have a stepping geometry and similar dip directions, forming an asymmetric rift basin with a faulted margin and a hinged margin. **B)** Border faults have a stepping geometry and convergent dip directions, causing the faulted and hinged margins to shift from side to side of the rift basin. **C)** Border faults are parallel, overlapping, and have similar dip directions, forming a platform. **D)** Border faults are parallel, overlapping, and have convergent dip directions, forming a symmetric rift basin with two faulted margins and no hinged margin. **E)** Border faults intersect.

faulted strata and basement. In some rift basins, the border faults are oblique-slip faults with both normal and strike-slip components of displacement. In these rift basins, many of the secondary normal faults strike obliquely to the trend of the border faults. For example, the trend of the faulted margin (and

the deep-seated border faults) of the Dampier rift basin is northeast–southwest. Most of the secondary normal faults in the sedimentary cover, however, strike north–south (Withjack and Eisenstadt, 1999) (Fig. 2D).

Flanks and Troughs

The footwall of each border fault is generally uplifted, producing an elevated rift flank (Figs. 4 and 5A) (e.g., Zandt and Owens, 1980; Jackson and McKenzie, 1983; King and Ellis, 1990; Anders and Schlische, 1994). Similarly, the hanging wall of each border fault is generally depressed, producing a trough (Figs. 4 and 5A). The magnitude of the footwall uplift and hanging-wall subsidence is greatest near the border fault and decreases away from the border fault into the footwall and hanging-wall blocks, respectively (e.g., Barnett et al., 1987) (Fig. 5B). It also decreases toward the tips of the border fault (e.g., Jackson and McKenzie, 1983; Anders and Schlische, 1994) (Fig. 5C). The ratio of footwall uplift to hanging-wall subsidence varies significantly, ranging from 1:1 to 1:10 (e.g., Jackson and McKenzie, 1983; Stein et al., 1988; Anders and Schlische, 1994).

Most rift basins are composed of several troughs separated by intrabasin highs (Fig. 4). The arrangement of the troughs and
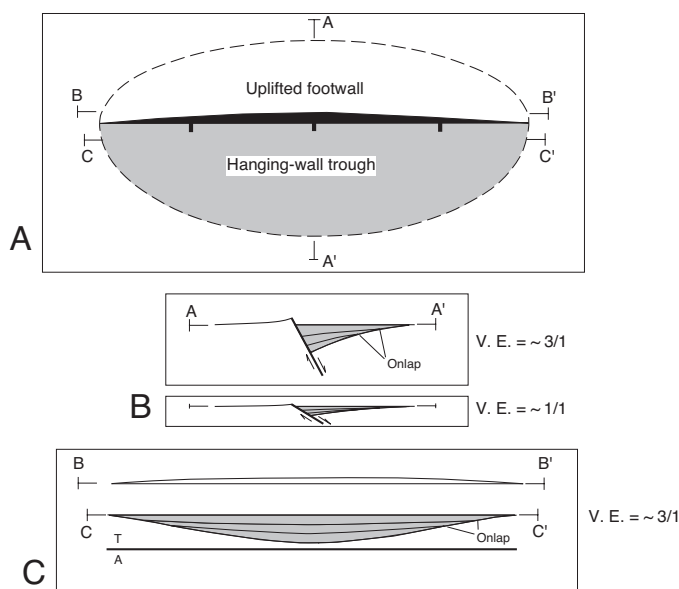

FIG. 5.—Footwall uplift and hanging-wall subsidence associated with border faults. **A)** Map view of a single border fault. The black line is a fault scarp; the line thickness indicates the displacement magnitude. **B)** Traverse section A–A' (with and without vertical exaggeration). The magnitude of the footwall uplift and hanging-wall subsidence decreases away from the border fault. Sedimentary units thicken toward the fault and progressively onlap the prerift units. **C)** Longitudinal sections. Longitudinal section B–B' shows that footwall uplift decreases toward the fault tips. Longitudinal section C–C' shows that hanging-wall subsidence decreases toward the fault tips. Sedimentary units thicken toward the center of the basin and progressively onlap the prerift units. The black line beneath the basin fill is a strike view of the border fault. T is motion toward the reader; A is motion away from the reader. Modified from Gibson et al. (1989) and Schlische (1995).

highs depends on the arrangement of the border faults. If the border faults have a stepping geometry and the same dip direction, then a series of adjacent troughs and highs develops on the faulted margin of the rift basin (Fig. 4A). If the border faults have a stepping geometry and convergent dip directions, then a series of offset troughs separated by intrabasin highs develops on opposing sides of the rift basin (Fig. 4B). If the border faults are parallel, overlapping, and have the same dip direction, then a series of parallel troughs and highs develops on the faulted margin of the rift basin (Fig. 4C).

Large-Scale Intrabasin Fault Blocks

Most rift basins are dissected by large-scale intrabasin faults (i.e., faults with displacements of more than several hundred meters and lengths of tens of kilometers) (Figs. 1 and 2). These intrabasin faults can strike parallel or obliquely to the trend of the border faults, and they can have normal and/or strike-slip components of displacement. Experimental studies suggest that the orientation and displacement on these intrabasin faults is controlled, in part, by the obliquity of the maximum extension direction relative to the rift-basin trend (Withjack and Jamison, 1986; Tron and Brun, 1991; Clifton et al., 2000) (Fig. 6). For orthogonal extension, intrabasin faults are likely to strike parallel to the rift trend and perpendicular to the maximum extension direction and have normal displacements (Fig. 6A). For oblique extension, intrabasin faults are likely to strike obliquely to the rift trend and subperpendicular to the maximum extension direction and have mostly normal displacement (Figs. 6B and 6C).

Large-Scale Transfer Zones

We define large-scale transfer zones as zones that accommodate the transfer of extension from one set of large-scale normal faults to another set of large-scale normal faults. Large-scale transfer zones affect most rift basins (e.g., Rosendahl, 1987; Morley et al., 1990; Faulds and Varga, 1998) (Fig. 7). In some cases, the deformation is focused, consisting one or two strike-slip or oblique-slip faults. In other cases, the deformation is diffuse, consisting of flexures and numerous normal, strike-slip, and oblique-slip faults. Experimental models (e.g., Clifton et al., 2000) and field studies (e.g., Moustafa, 1997) suggest that the deformation within large-scale transfer zones is more likely to be focused if the magnitude of extension is large, the sedimentary cover is thin, and/or the sedimentary cover contains limited salt or shale. Thus, a transfer zone can narrow through time (as the magnitude of extension increases) or along strike (as the thickness of the sedimentary cover decreases).
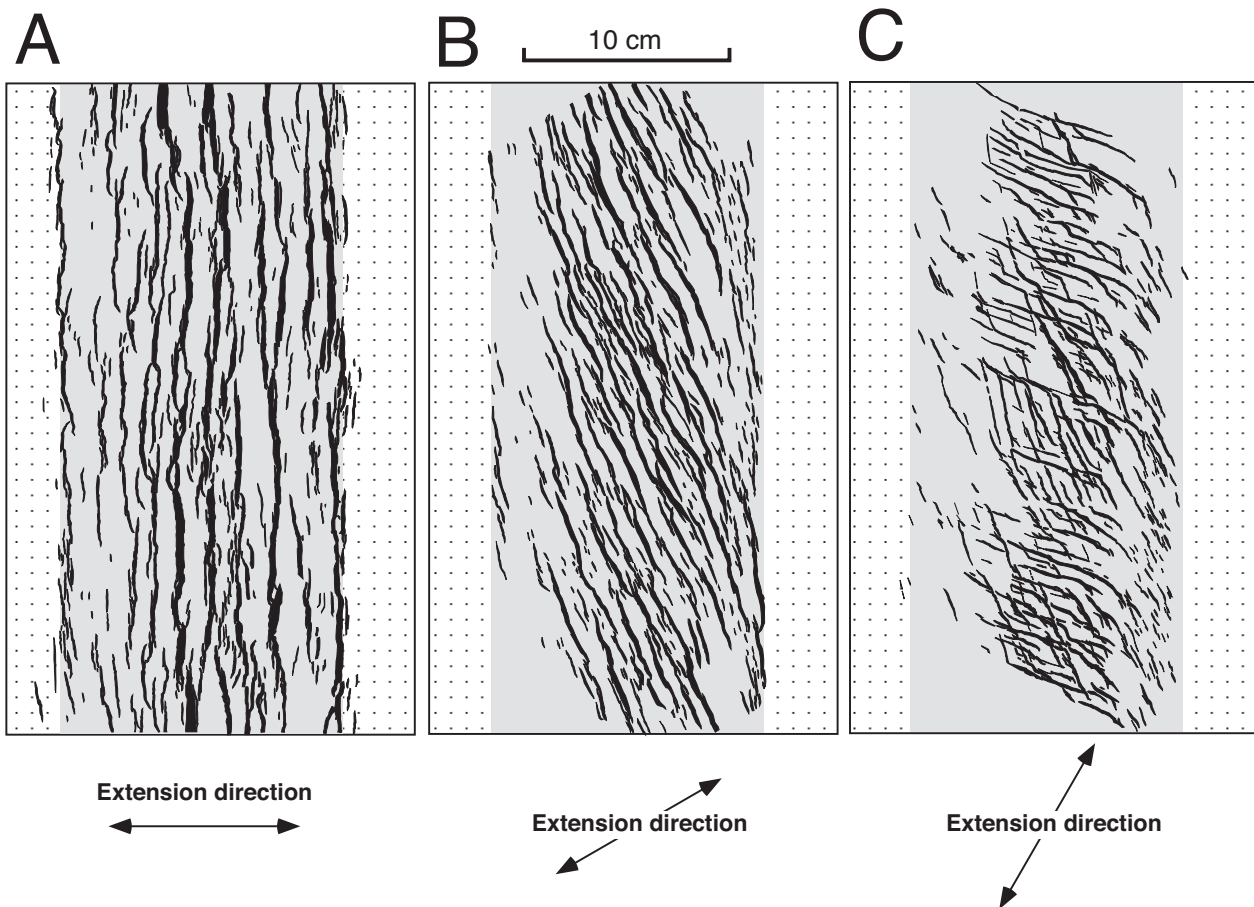

FIG. 6.—Surface fault patterns for orthogonal and oblique rifting based on experimental (clay) models (after Clifton et al., 2000). The rift axis is vertical. Gray areas are extended regions; dotted areas are regions with no extension. **A)** Orthogonal extension with the displacement direction perpendicular to the rift axis. **B)** Oblique extension with the displacement direction 60° from the rift axis. **C)** Oblique extension with the displacement direction 30° from the rift axis.
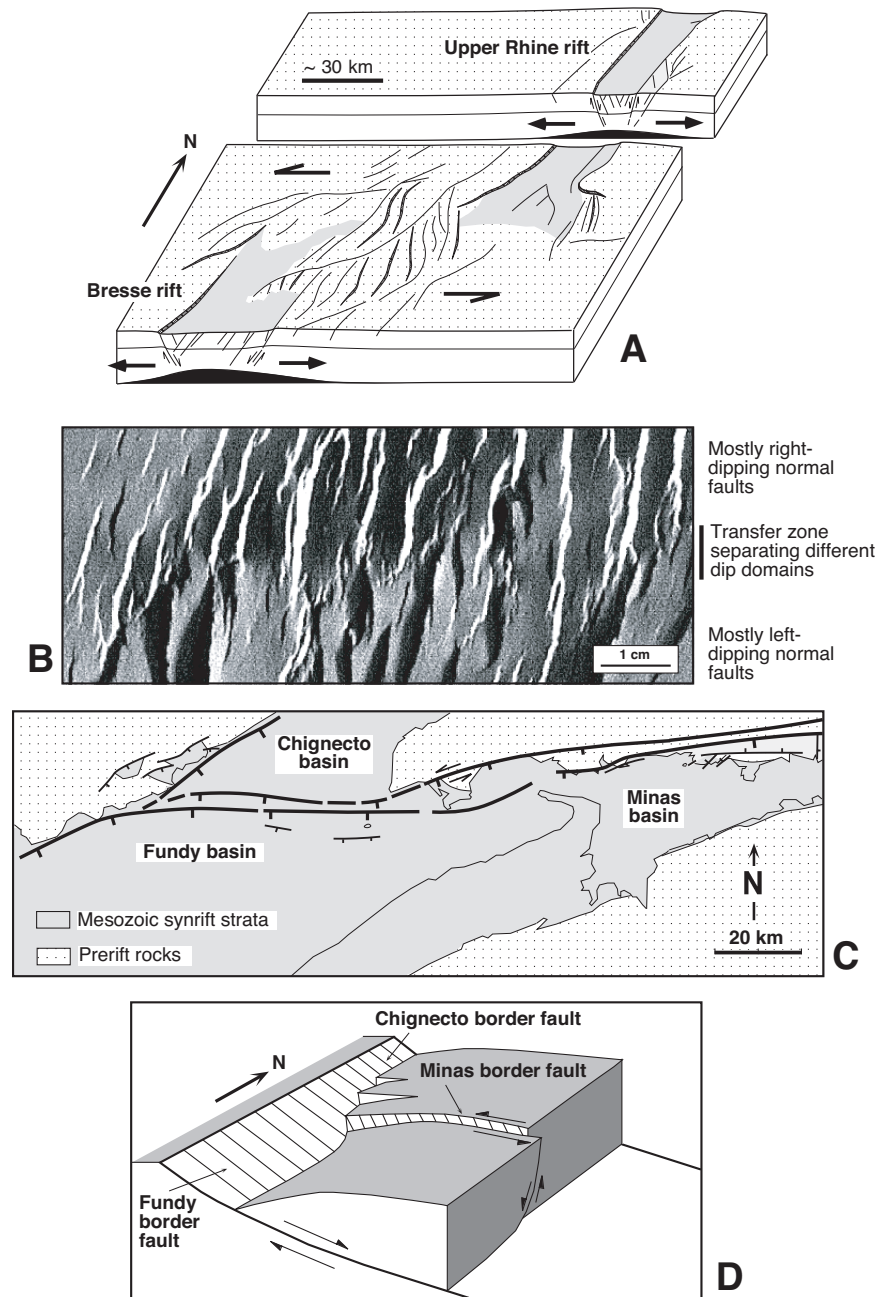
FIG. 7.—Large-scale transfer zones. **A)** Block diagram of a transfer zone that links laterally offset zones of extension. This broad transfer zone, composed of numerous normal, strike-slip, and oblique-slip faults, links the northern end of the Bresse rift basin with the southern end of the Upper Rhine rift basin (after Illies, 1977). **B)** Map view of a model of distributed extension in homogeneous clay. A transfer zone developed between regions with normal faults with different dip directions and locations (after Clifton et al., 2000). **C)** Map view of a transfer zone that separates regions with different amounts of extension. An east-trending oblique-slip fault zone forms the northern border of Minas rift basin. This zone separates the Chignecto rift basin (less extension) from the Fundy rift basin (more extension) (after Withjack et al., 1995b). **D)** Schematic block diagram showing the geometries of the border faults in the Fundy, Chignecto, and Minas rift basins.

One type of large-scale transfer zone connects stepped zones of extension. The intrabasin highs between stepping border faults with convergent dip directions are examples of this type of transfer zone (Fig. 4B). A much larger-scale example of this type of transfer zone is the zone of distributed deformation that links

the northern end of the Bresse rift basin with the southern end of the Upper Rhine rift basin (Contini and Theobald, 1974; Angelier and Bergerat, 1983; Fig. 7A). A second type of large-scale transfer zone separates regions in which the normal faults have different dip directions and locations. Examples include the zones that

bound the three dip provinces of the Suez rift basin (Moustafa, 1976; Thiebaud and Robson, 1979; Colletta et al., 1988; Fig. 2C). In each of these dip provinces, the dip directions of the normal faults and strata differ from those in the adjacent dip province(s). Experimental models of distributed extension with a homogeneous modeling material have produced similar transfer zones (Clifton et al., 2000) (Fig. 7B). A third type of large-scale transfer zone separates regions with different amounts of extension. For example, the east-striking oblique-slip fault zone on the northern margin of the Minas rift basin is a transfer zone that separates the Fundy rift basin from the less-extended Chignecto rift basin (Figs. 7C and 7D).

FAULTS

Normal Faults

Normal faults are the most common structures within rift basins. Many normal faults are deep-seated, involving the crystalline basement (Fig. 8A). Others detach into salt or shale above the basement (Fig. 8B). Examples of basement-involved normal faults include the border faults of the Newark, Fundy, Jeanne d'Arc, and Suez rift basins (Figs. 1A–C, E). Examples of detached normal faults include the small-scale normal faults that die out within salt within the Jeanne d'Arc, Suez, and and Vøring rift basins (Figs. 1C, E, and F).

In cross section, the geometries of normal faults vary considerably (Fig. 1). Some normal faults are planar, whereas other normal faults are listric. Some normal faults have steep dips (e.g., most normal faults within the Upper Rhine and Suez rift basins), whereas other normal faults have gentle to moderate dips (e.g., the border faults of the southern Newark, Fundy, and Jeanne d'Arc rift basins). Several processes can produce low-angle normal faults. Reactivation of gently dipping zones of weakness creates low-angle normal faults. For example, the Mesozoic reactivation of Paleozoic thrust faults produced many of the low-angle normal faults in the Newark and Fundy rift basins (Plint and van de Poll, 1984; Ratcliffe et al., 1986; Withjack et al., 1995b). "Domino-style" rotation of fault blocks increases stratal dips and decreases fault dips (e.g., Proffett, 1977). For example, 30° of "domino-style" rotation increases stratal dips from 0° to 30° and decreases fault dips from 60° to 30°. Compaction commonly alters the cross-sectional shapes of normal faults. Compaction causes fault dips to decrease as burial depth increases (Roux, 1979; Davison, 1987; Xiao and Suppe, 1989).

In map view, most normal faults have a sinuous appearance and trend subperpendicular to the direction of maximum extension (Fig. 2). Numerical and experimental models suggest that this characteristic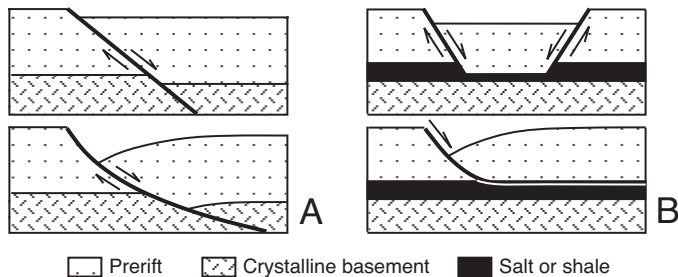 map pattern forms during fault-population evolution (Cowie et al., 1995; Cowie, 1998; Marchal et al., 1998; Ackermann et al., 2001). During the early stages of normal faulting, numerous minor normal faults form; these trend subperpendicular to the direction of maximum extension (Fig. 9A). They are isolated, "lens-shaped" structures with maximum displacements near their centers and no displacement at their ends. Examples include centimeter-scale normal faults in the Danville rift basin (Schlische et al., 1996) and meter- to kilometer-scale minor normal faults in the Volcanic Tableland, California, of the Basin-and-Range province (Dawers et al., 1993) and the Kenya rift basin (Chapman et al., 1978) (see Fig. 11). During subsequent stages of normal faulting, fault displacements and lengths increase (Figs. 9B and C). Some of the minor normal faults that formed during the early stage coalesce, forming sinuous normal faults with greater displacements and lengths. This linkage process continues as extension increases, producing a few major, through-going
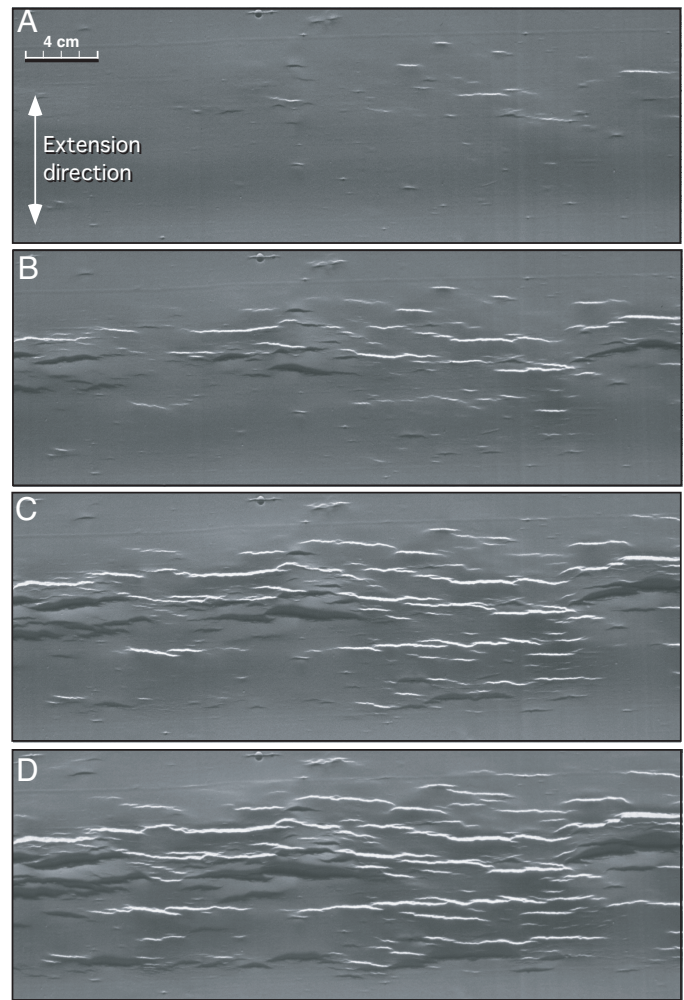
FIG. 9.—Development of normal faults in map view. Photos show faults cutting the upper surface of a homogeneous clay layer deformed above a uniformly extended rubber sheet. The amount of extension of the rubber sheet is **A)** 1.5 cm, **B)** 1.75 cm, **C)** 2.0 cm, and **D)** 2.25 cm. The bright faults dip toward the light source (bottom of image), and the dark faults dip away from the light source. The majority of the faults begin as isolated features. Linkage of adjacent faults results in complex fault traces.

FIG. 8.—Schematic cross sections of **A)** basement-involved and **B)** detached normal faults. Either type of normal fault can be planar or listric.

normal faults (Fig. 9D). Many of the faults not involved in the linkage process either stop growing entirely or grow at a slower rate. Because major normal faults are composed of linked minor normal faults, fault displacements, trends, and dips can vary considerably along strike (Fig. 9D).

Strike-Slip, Oblique-Slip, and Reverse Faults

Strike-slip, oblique-slip, and reverse faults also form within rift basins. Strike-slip and oblique-slip faults are most common in large-scale transfer zones (e.g., Rosendahl, 1987) and in rift basins produced by oblique extension (e.g., Withjack and Jamison, 1986) (Figs. 6B, 6C, and 7). Experimental models show that reverse faults can develop as steeply dipping normal faults propagate to the surface (Fig. 10A; Horsfield, 1977; Vendeville, 1987; Withjack and Callaway, 2000). Reverse faults in the Suez rift basin might be analogous to those observed in these models (Fig. 10B; Patton, 1984; Gawthorpe et al., 1997). Some reverse faults in rift basins are actually rotated normal faults. For example, strata and normal faults rotated up to 70° during the past 30 million years in the Lemitar Mountains of the Rio Grande rift basin (Chamberlin, 1983) (Fig. 10C). This large rotation caused some initially high-angle, west-dipping normal faults to become high-angle, east-dipping reverse faults. Finally, reverse faults are common in inverted rift basins, (e.g., Cooper and Williams, 1989). These reverse faults form after rifting, and many are reactivated normal faults. For example, normal faults reactivated with reverse displacement exist in the Fundy rift basin (Fig. 1B), the Viking rift basin (Fig. 1G), and the Sunda arc rift basins (Fig. 10D).

FOLDS

Three types of folds are genetically associated with normal faulting: fault-displacement folds, fault-propagation folds, and fault-bend folds (e.g., Figs. 11–14; Hamblin, 1965; Withjack and Drickman Pollock, 1984; Schlische, 1995; Janecke et al., 1998). As discussed below, the geometry referred to in the literature as "normal-drag" folding (i.e., the hanging-wall beds dip away from the normal fault) is generally produced by fault-propagation folding and/or fault-bend folding. The geometry referred to in the literature as "reverse-drag" folding (i.e., the hanging-wall
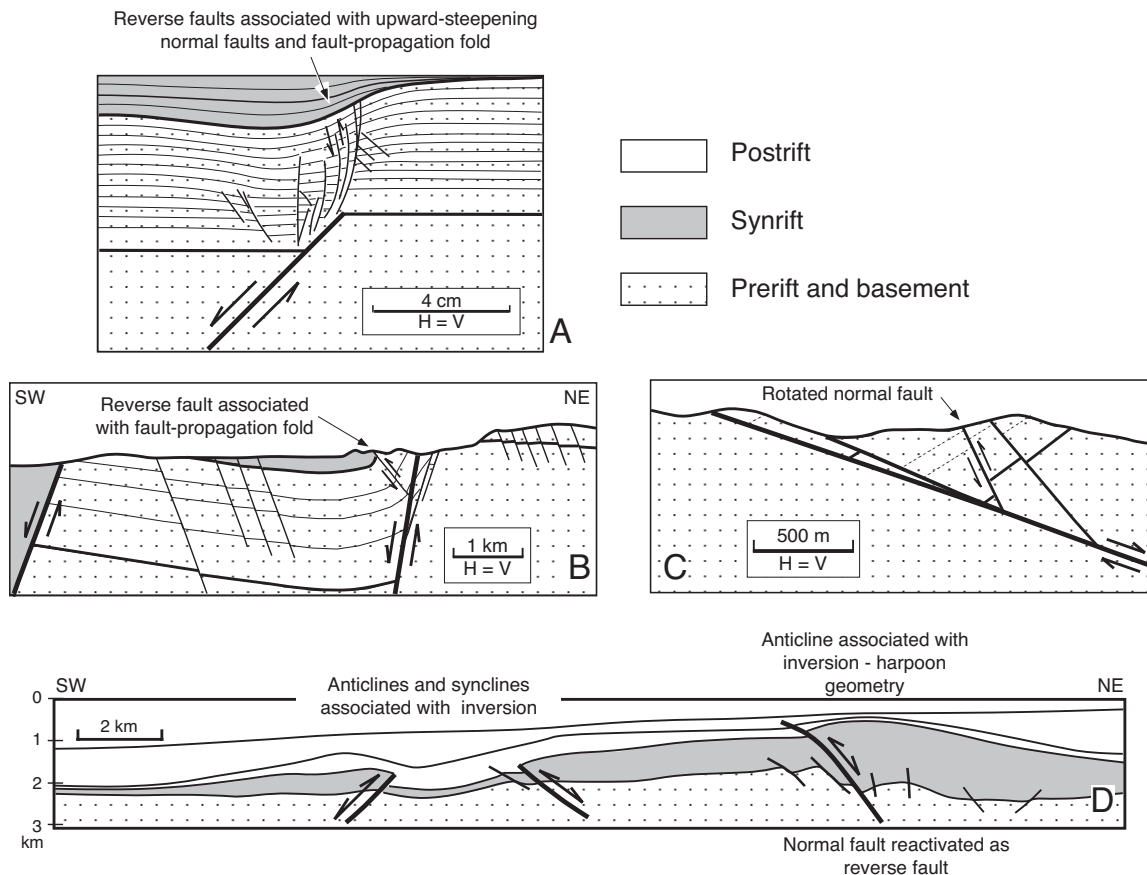

FIG. 10.—Reverse faults associated with rifting. **A)** Line drawing of a clay model showing steeply dipping reverse faults associated with an upward-propagating normal fault (after Withjack and Callaway, 2000). **B)** Example of a reverse fault associated with fault-propagation folding in the Suez rift basin (after Gawthorpe et al., 1997). This reverse fault may be analogous to those in the experimental models. **C)** Rotated normal fault from the Lemitar Mountains of the Rio Grande rift basin (after Chamberlin, 1983). Strata and normal faults rotated up to 70°, causing some initially high-angle, west-dipping normal faults to become high-angle, east-dipping reverse faults. **D)** Normal faults reactivated with reverse displacement in inverted rift basins from the Sunda arc. During basin inversion, some normal faults became reverse faults, producing synclines and anticlines with harpoon geometries (after Letouzey, 1990).
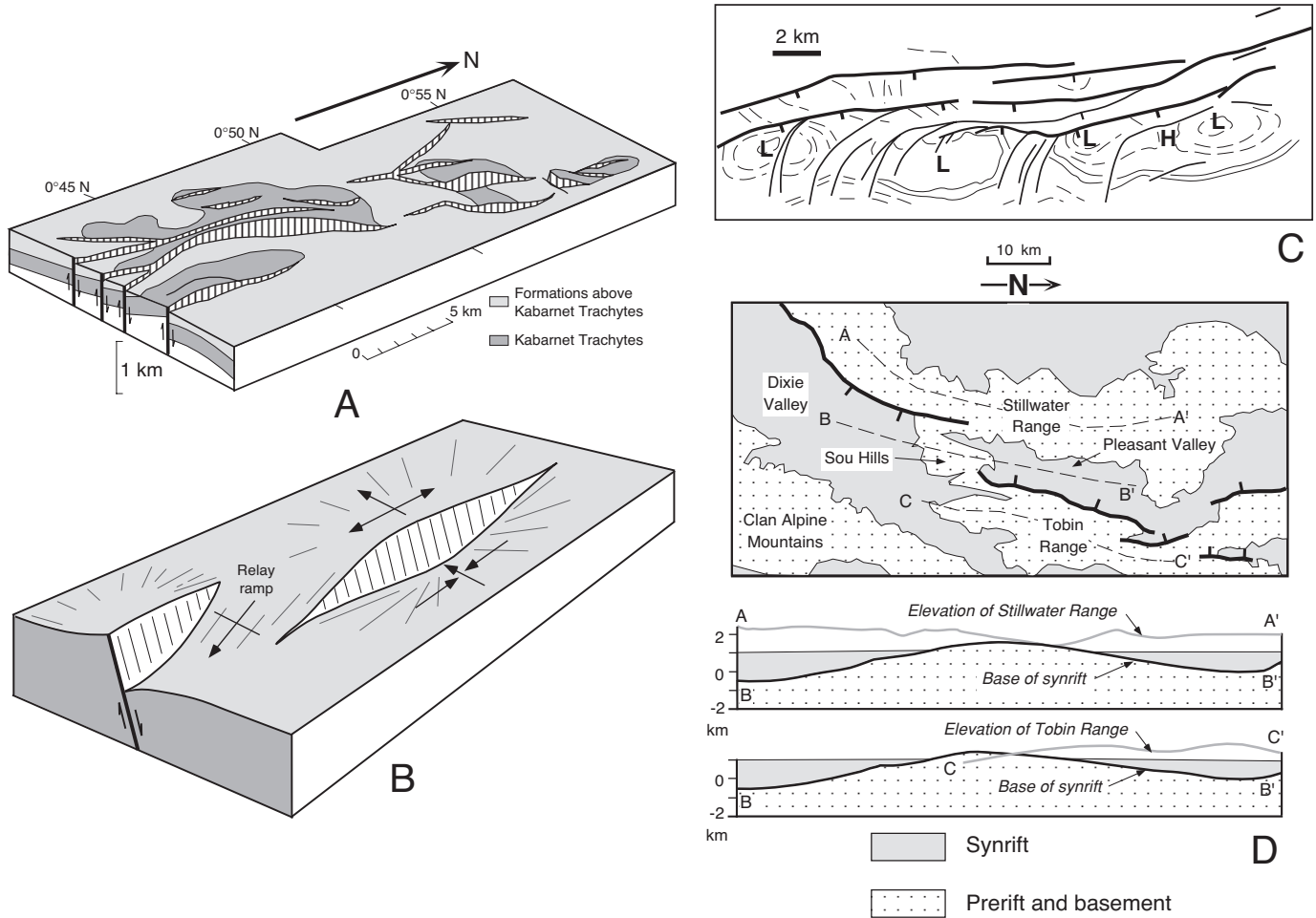
Fig. 11.—Examples of fault-displacement folds. **A)** Fault-displacement folds in the Kenya rift basin (after Chapman et al., 1978). Footwall uplift is greatest where fault displacement is greatest, exposing the underlying Kabarnet Trachytes. **B)** Fault-displacement folds and relay ramp associated with stepping normal faults. **C)** Line drawing of a time slice from 3D seismic survey from southeast Asia showing relative highs (H) and lows (L) in hanging-wall of normal faults. **D)** Fault-displacement folds associated with normal faults in the Basin and Range rift system (after Zhang et al., 1991; Jackson and Leeder, 1994). *Top:* Geologic map of the Dixie Valley–Pleasant Valley fault system of Nevada. *Bottom:* Longitudinal profiles of footwall uplift and hanging-wall subsidence along three transects indicated in the upper panel. The Sou Hills is an interbasin high associated with footwall elevation lows in the Stillwater and Tobin Ranges.

beds dip toward the normal fault) is generally produced by fault-displacement folding and/or fault-bend folding.

Fault-Displacement Folds

We define fault-displacement folds as flexures produced by changes in fault displacement (Fig. 11). The axes of some fault-displacement folds are subparallel to the associated fault; they form because the displacement decreases with increasing distance from a normal fault (Fig. 5B). This displacement geometry leads to monoclinal upfolding in the footwall block (i.e., footwall uplift) and monoclinal downfolding (i.e., "reverse-drag") in the hanging-wall block (e.g., Zandt and Owens, 1980; Barnett et al., 1987). The axes of other fault-displacement folds are subperpendicular to the associated fault; they form because the displacement varies along the strike of a normal fault (Walsh and Watterson, 1987) (Fig. 5C). Several factors produce displacement variations along strike: fault segmentation during the early stages

of faulting, linkage during the later stages of faulting, and/or fault-surface irregularities. These fault-displacement folds include the hanging-wall synclines and footwall anticlines that form where fault displacements are greatest (Fig. 11B) and the footwall synclines and hanging-wall anticlines that form where fault displacements are least. As shown below, fault-displacement folding produces three-dimensional culminations and depressions in the footwalls and hanging walls of many normal faults.

Fault-displacement folds form at all scales. At the small scale, folds in the footwalls and hanging walls of normal faults in the Kenya rift basin of East Africa are produced by fault-displacement folding (Chapman et al., 1978; Fig. 11A). Relay ramps (e.g., Goguel, 1962; Kelley, 1979; Larsen, 1988; Peacock and Sanderson, 1991, 1994) are fault-displacement folds that form between stepping normal faults that dip in the same direction. These folds connect the hanging-wall block of one fault with the footwall block of the other fault (Fig. 11B). Fault-
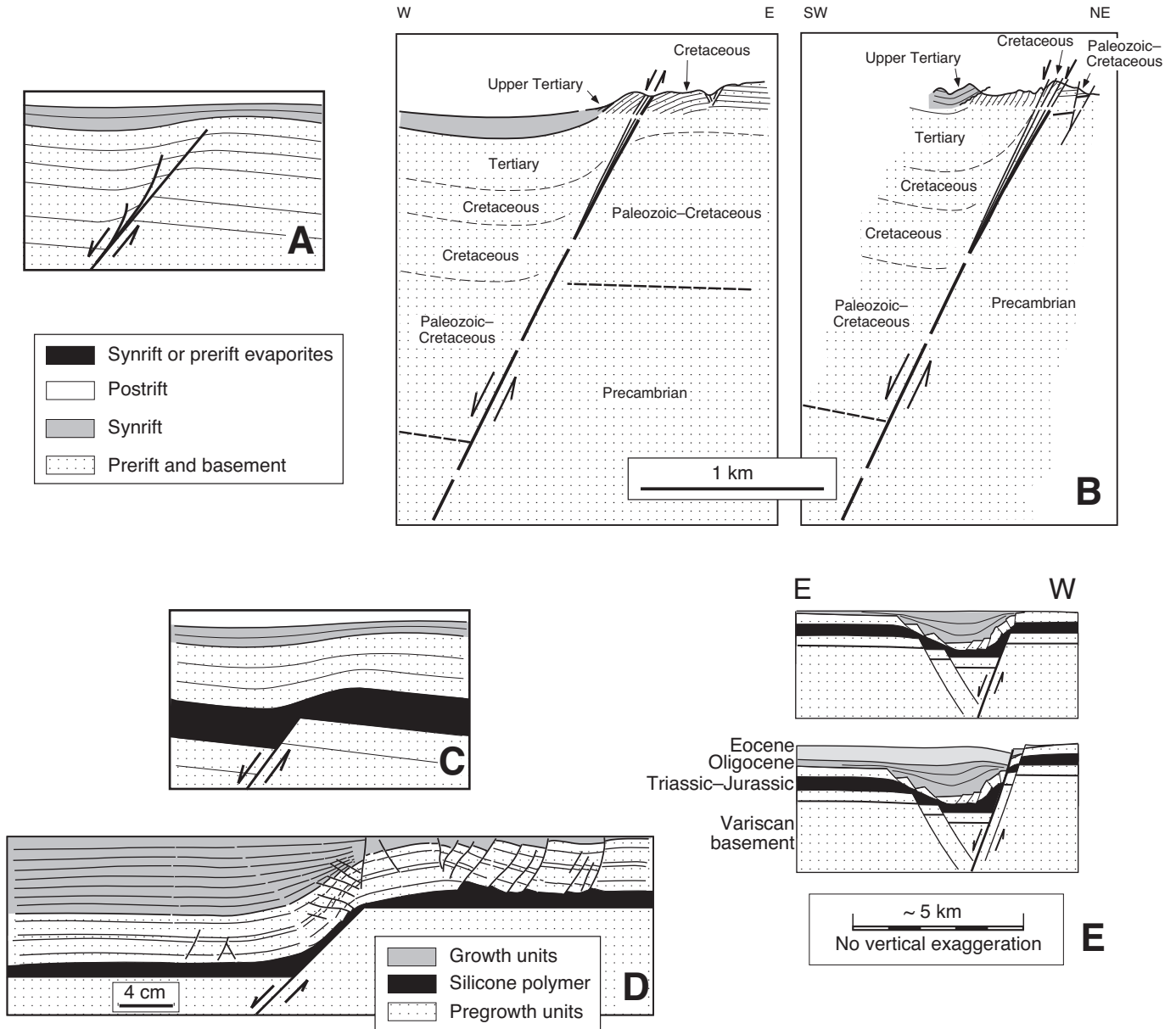
Fig. 12.—Extensional fault-propagation and forced folds. **A)** Sketch of an extensional fault-propagation fold with smooth upward transition from faulting to folding. **B)** Extensional fault-propagation folds from the Suez rift basin (after Patton, 1984; Withjack et al., 1990). **C)** Sketch of an extensional forced fold with abrupt upward transition from faulting to folding. Presence of salt facilitates development of extensional forced folds. **D)** Line drawing of clay–putty model of an extensional forced fold (after Withjack and Callaway, 2000). The black area is silicone putty deposited before faulting. The dotted pattern below the putty represents aluminum blocks; the dotted pattern above the putty is clay deposited before faulting. The gray area is clay deposited during faulting. **E)** An extensional forced fold from the eastern margin of the Rhine rift basin (after Maurin, 1995). *Top*: A deep-seated normal fault has not propagated through the sedimentary section. *Bottom*: A deep-seated normal fault has propagated through the sedimentary section.

displacement folds are evident on time slices from 3D seismic surveys, appearing as anticlinal highs and synclinal lows in the footwalls and hanging walls of normal faults (Fig. 11C). The residual intrabasin highs between stepping border faults with convergent dip directions are large-scale fault-displacement folds (as well as transfer zones) (Figs. 4D and 11D). Finally, at the largest scale, the uplifted flank and the depressed trough of a rift basin are produced by fault-displacement folding associated with the border fault (Fig. 5).

Extensional Fault-Propagation Folds and Forced Folds

Folds commonly develop above upward-propagating normal faults. If the vertical transition from fault- to fold-dominated
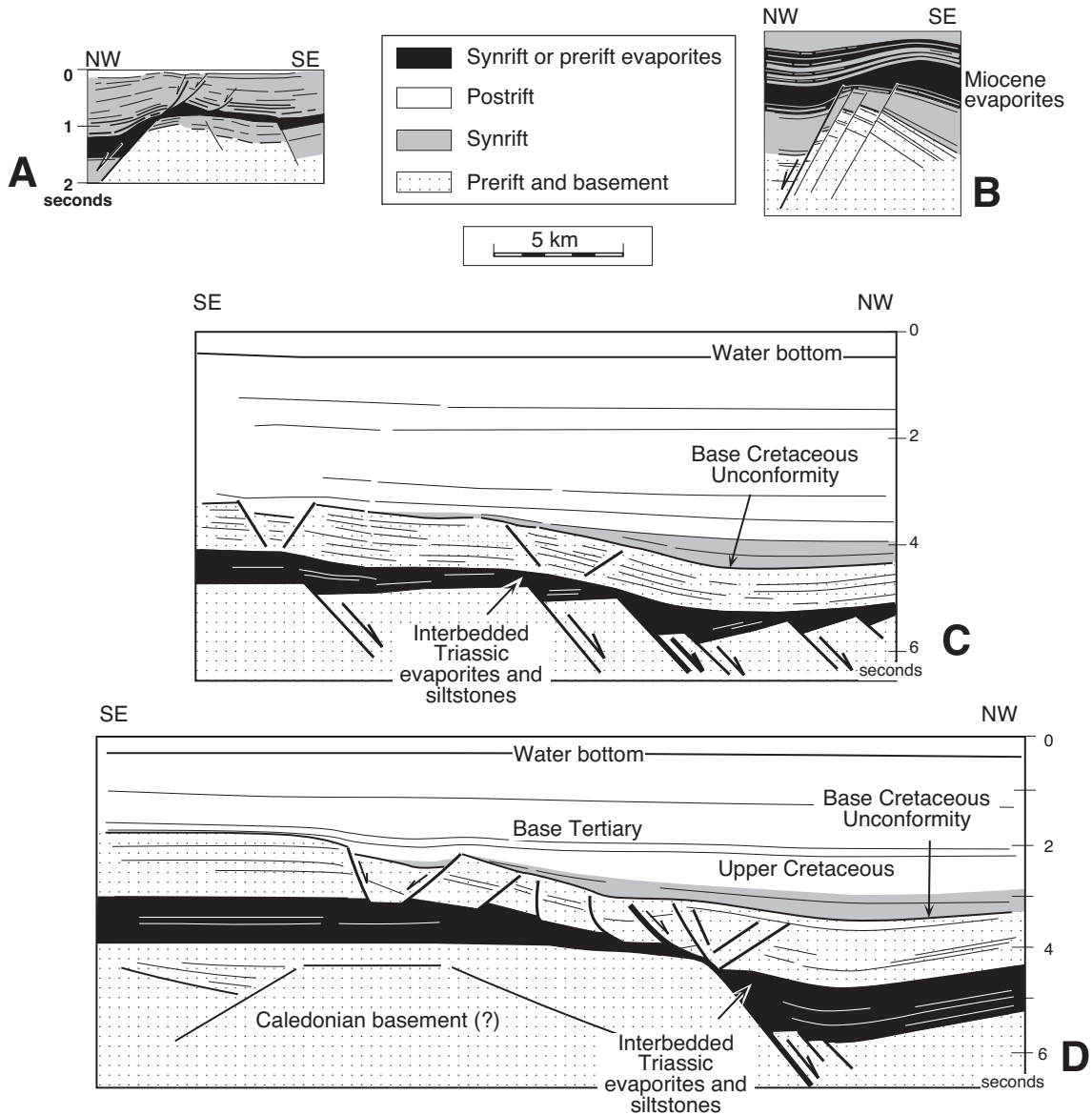
F<small>IG</small>. 13.—Examples of extensional forced folds from the Suez and Vøring rift basins. All sections have the same horizontal scale. Geologic cross sections are displayed without vertical exaggeration. Seismic sections are displayed without vertical exaggeration assuming a velocity of 4 km/s; vertical axes are in seconds of two-way travel time. **A)** Line drawing of a seismic section from the Suez rift basin (after Patton et al., 1994; Withjack and Callaway, 2000). **B)** Geologic cross section through the Ramadan oil field in the Suez rift basin (after Brown, 1980; Withjack and Callaway, 2000). **C)** Line drawing of a time-migrated seismic section (NRGS84-407) across the Smørbukk structure, offshore Norway (after Withjack et al., 1989; Withjack et al., 1990; Withjack and Callaway, 2000). **D)** Line drawing of a time-migrated seismic section (GMNR94-310) across the Mikkel structure, offshore Norway (from Withjack and Callaway, 2000).

deformation is smooth, we call these folds extensional fault-propagation folds (Fig. 12A). If the vertical transition from fault- to fold-dominated deformation is abrupt, we call these folds extensional forced folds (Fig. 12C). The presence of subsurface evaporites and overpressured shales facilitates the development of extensional forced folds by decoupling the shallow, folded strata from the deep, faulted strata and basement (Laubscher, 1982; Vendeville, 1987; Withjack et al., 1989; Withjack et al., 1990; Maurin, 1995; Withjack and Callaway, 2000).

Examples of extensional fault-propagation folds occur in the prerift and synrift packages above the faulted crystalline basement of the Suez rift basin (Robson, 1971; Garfunkel and Bartov, 1977; Thiebaud and Robson, 1979, 1981; Brown, 1980; Patton, 1984; Coffield and Schamel, 1989; Gawarecki and Coffield, 1990) (Figs. 10B and 12B). The folds in the Paleozoic through Eocene prerift strata are relatively narrow flexures with steeply dipping beds. Secondary faults associated with the fault-propagation folding include upward-steepening normal and reverse faults
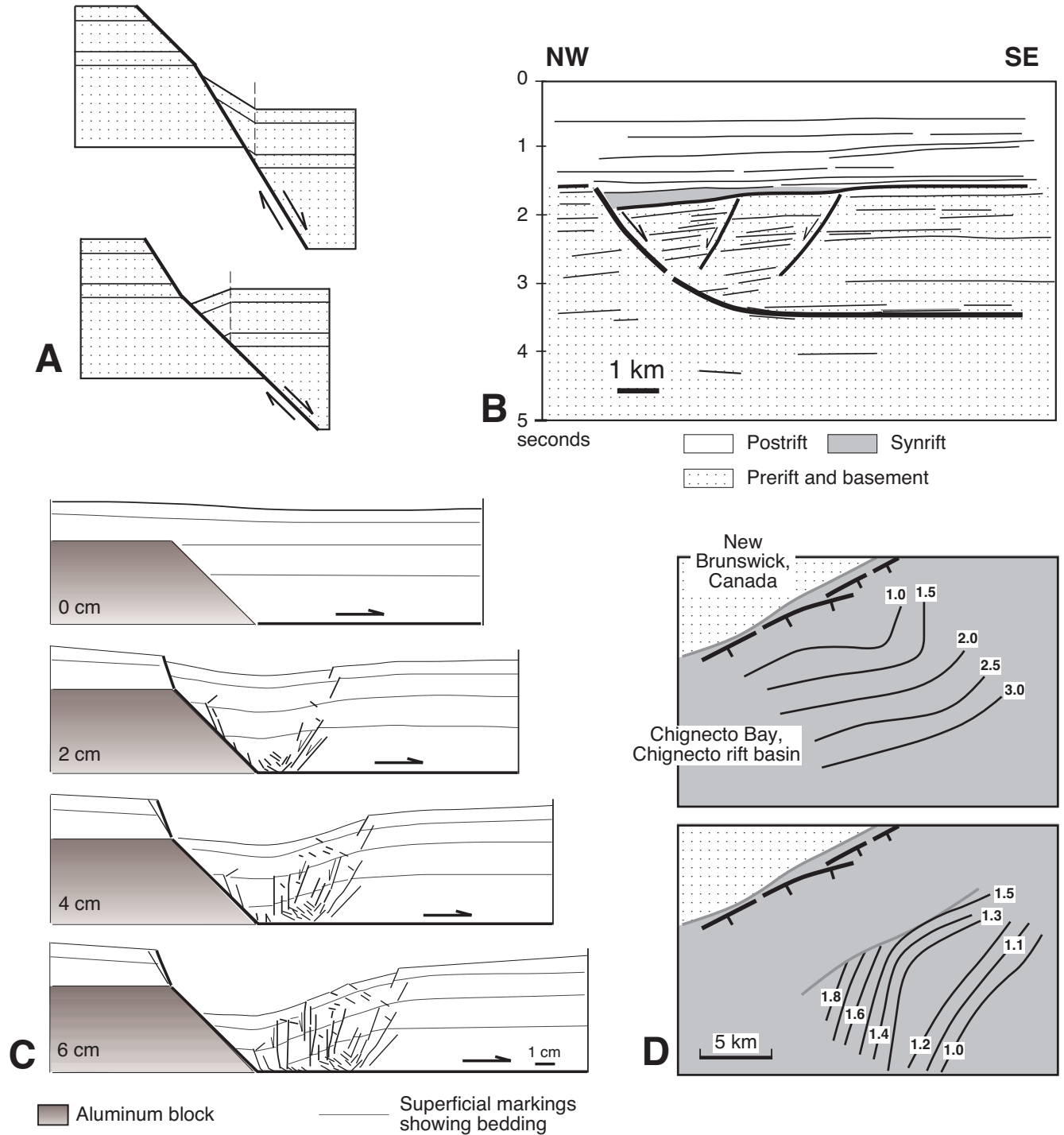
FIG. 14.—Extensional fault-bend folds. **A)** Geometric models of extensional fault-bend folds (with vertical shear as the deformation mechanism) produced by changes in fault dip with depth. **B)** Line drawing of a seismic section showing an extensional fault-bend fold from the Vøring rift basin (after Withjack and Peterson, 1993). The normal fault has a listric shape and detaches within Triassic salt. Hanging-wall strata dip toward the normal fault, and secondary normal faults emanate from the fault bend. **C)** Line drawing of a clay model showing the evolution of an extensional fault-bend fold (after Withjack et al., 1995a). **D)** Extensional fault-bend fold related to variation in fault shape along strike. *Top:* Contours (in seconds of two-way travel time) on the surface of the border fault of the Chignecto rift basin. Note the "bump" on the fault surface. *Bottom*: Contours (in seconds of two-way travel time) on a prominent synrift reflection. The gray line is the hanging-wall cut off. This hanging-wall fold is an extensional fault-bend fold related to the "bump" on the surface of border fault of the Chignecto rift basin.

(e.g., Patton, 1984; Gawthorpe et al., 1997; Fig. 10B). The extensional fault-propagation folds in the Suez rift basin resemble those from single-layer experimental models (Withjack et al., 1990; Withjack and Callaway, 2000) (Fig. 10A).

Examples of extensional forced folds are found along the eastern and western margins of the Upper Rhine rift basin (Fig. 12E; Laubscher, 1982; Maurin, 1995), in the Suez rift basin (Figs. 13A and 13B; Withjack and Callaway, 2000), and throughout the Haltenbanken area of offshore Norway (Figs. 13C and 13D; Withjack et al., 1989; Withjack et al., 1990). In the Haltenbanken area, the extensional forced folds affect Triassic, Jurassic, and Cretaceous strata above Triassic evaporites. The evaporites separate folded strata from underlying faulted strata and crystalline basement. These forced folds are several kilometers wide and have up to several kilometers of structural relief. Narrow, detached grabens formed near the anticlinal axial surfaces of many of these forced folds (Withjack and Callaway, 2000). The extensional forced folds in the Haltenbanken area resemble those from multi-layer experimental models (Vendeville, 1987; Withjack and Callaway, 2000) (Fig. 12D).

Extensional Fault-Bend Folds

Extensional fault-bend folds are flexures that form in the hanging walls of nonplanar normal faults (e.g., Xiao and Suppe, 1992). Simple geometric models, assuming that rock volume remains constant during folding, show how the shape of a normal fault influences the shape of the fault-bend fold in its hanging wall (Fig. 14A). If the surface of a normal fault has a gently dipping upper segment and a steeply dipping lower segment, the geometric models show that a monocline forms in the hanging wall of the normal fault (Fig. 14A, top). The folded strata dip away from the fault (i.e., "normal-drag" folding). If the surface of a normal fault has a steeply dipping upper segment and a gently dipping lower segment, the models show that a monocline also forms in the hanging wall of the normal fault (Fig. 14A, bottom). The folded strata, however, dip toward the fault (i.e., "reverse-drag" folding). Experimental models and seismic examples of this latter type of fault-bend fold suggest that secondary normal faults commonly dip toward the main fault and emanate from the fault bend (e.g., Figs. 14B and 14 C; Withjack and Peterson, 1993; Withjack et al., 1995a).

Variations in fault shape along strike also produce extensional fault-bend folds. Unlike more typical fault-bend folds whose axes are parallel to the master normal fault, the axes of these folds are perpendicular to the master normal fault. These fault-bend folds resemble fault-displacement folds. For example, a gentle anticline has formed in the hanging-wall strata above a pronounced "bump" on the surface of the border fault of the Chignecto rift basin (Fig. 14D). The fold axis is roughly perpendicular to the boundary fault.

RIFT-BASIN STRUCTURAL STYLES

Four factors strongly influence the structural styles of rift basins: the mechanical behavior of the prerift and synrift packages, the tectonic activity before rifting, the obliquity of rifting, and the tectonic activity after rifting. On the basis of these factors, we have defined a standard rift basin and four end-member variations to provide a framework for understanding the variety of structural styles in rift basins (Fig. 15). The standard rift basin has little salt or shale in the prerift or synrift packages. Few preexisting zones of weakness in the prerift strata or crystalline basement were reactivated during rifting, and little tectonic activity followed rifting. The standard rift basin is characterized by moderately to steeply dipping basement-involved normal faults that strike roughly perpendicular to the direction of maximum extension (Fig. 15A). Type 1 rift basins have salt or thick shale in the prerift and/or synrift packages, facilitating the decoupling of the shallow and deep deformation (Fig. 15B). Type 1 rift basins are characterized by extensional forced folds above basement-involved normal faults and detached normal faults and associated fault-bend folds. In Type 2 rift basins, contractional activity before rifting produced low-angle thrust faults in the prerift strata and/or crystalline basement (Fig. 15C). The reactivation of these contractional structures during rifting created the low-angle normal faults characteristic of Type 2 rift basins. In Type 3 rift basins, the preexisting zones of weakness in the prerift strata or crystalline basement strike obliquely to the direction of maximum extension, leading to oblique rifting (Fig. 15D). Type 3 rift basins are characterized by faults with strike-slip, normal, and oblique-slip displacement and with multiple trends (i.e., parallel to the rift trend and perpendicular to the direction of maximum extension). In Type 4 rift basins, one or more contractional events followed rifting (Fig. 15E). These inverted rift basins are affected by late-formed contractional structures including normal faults reactivated with reverse displacement, newly formed reverse faults, and contractional fault-bend and fault-propagation folds.

Most rift basins have attributes of the standard rift basin and one or more of the end-member variations. The Jeanne d'Arc rift basin of offshore maritime Canada has attributes of Type 1 and Type 2 rift basins with Triassic/Jurassic salt in the synrift package and major Paleozoic contraction preceding Mesozoic rifting (Fig. 1C). Many of the basement-involved normal faults in this rift basin are low-angle, Paleozoic thrust faults reactivated with normal displacement (e.g., Keen et al., 1987; de Voogd et al., 1990). Detached normal faults and forced folds formed in the sedimentary cover above several basement-involved normal faults during rifting (Withjack and Callaway, 2000). The Fundy rift basin of eastern North America has attributes of Types 2, 3, and 4 rift basins with one or more Paleozoic contractional events preceding Mesozoic rifting, oblique slip along the east-striking border fault of the Minas rift basin, and a Mesozoic contractional episode following rifting (Figs. 1B, 7C, and 7D; Withjack et al., 1995b). Many of the basement-involved normal faults in this rift basin are low-angle, Paleozoic thrust faults reactivated with normal displacement. After rifting, several of these basement-involved faults were reactivated again with reverse displacement, inverting the rift basin and folding the synrift strata. The Dampier rift basin of offshore northwest Australia has attributes of Type 1 and Type 3 rift basins with thick Triassic shale in the prerift package and oblique rifting during Mesozoic time (Figs. 1H and 2D). Forced folds developed in the sedimentary cover above some border faults. Many of secondary faults in the sedimentary cover strike obliquely to the trend of these border faults and subperpendicular to the extension direction (Withjack and Eisenstadt, 1999; Schlische et al., 2002).

STRATIGRAPHIC UNITS OF RIFT BASINS

Rift-Onset and Postrift Unconformities

The most basic stratigraphic units associated with rifting are the prerift, synrift, and postrift packages (Fig. 16A). The rift-onset unconformity separates the prerift and synrift packages. In many rift basins, the rift-onset unconformity is subtle. For example, detailed field studies in the Suez rift basin (Garfunkel and Bartov, 1977) and the Upper Rhine rift basin (Illies, 1977) indicate that, in these basins, limited uplift and erosion occurred during the early

Standard
- Little salt or shale in prerift or synrift
- Few preexisting zones of weakness reactivated during rifting
- Little tectonic activity after rifting
- Characterized by moderately to steeply dipping basement-involved normal faults that strike perpendicular to extension direction

A

Type 1
- Salt or thick shale in the prerift and/or synrift
- Characterized by extensional forced folds above basement-involved normal faults and detached normal faults and associated fault-bend folds
- Decoupling of shallow and deep deformation

B

Type 2
- Contractional activity before rifting produced low-angle thrust faults
- Reactivation of thrust faults during rifting created low-angle normal faults

C

Extension direction

Type 3
- Preexisting zones of weakness strike obliquely to extension direction, leading to oblique rifting
- Characterized by faults with strike-slip, normal, and oblique-slip displacement and with multiple trends (i.e., parallel to rift trend and perpendicular to extension direction)

D

Type 4
- One or more contractional events followed rifting, leading to basin inversion
- Characterized by late-formed contractional structures including normal faults reactivated with reverse displacement, newly formed reverse faults, and contractional fault-bend and fault-propagation folds

E

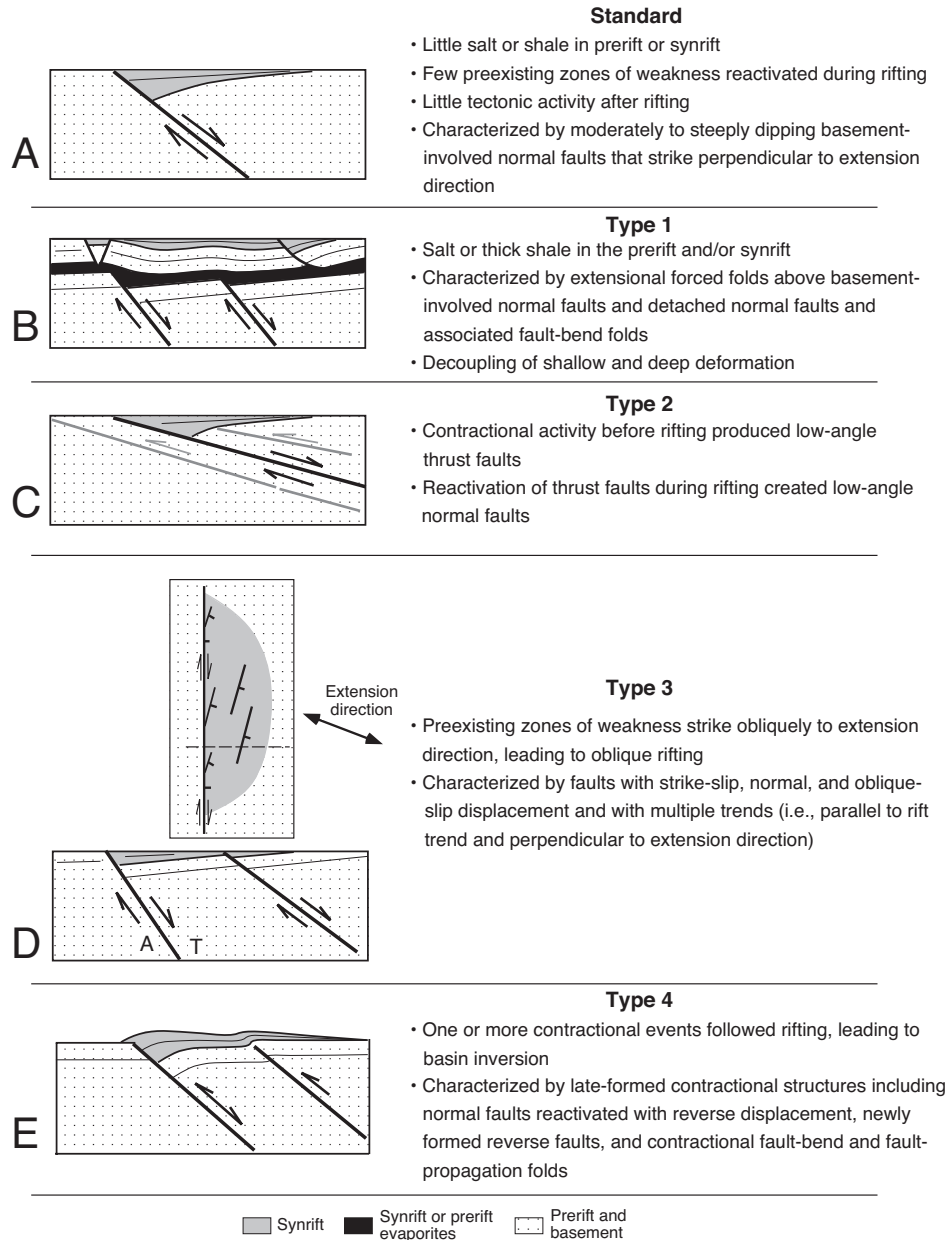Synrift | Synrift or prerift evaporites | Prerift and basement

FIG. 15.—Rift-basin structural styles. **A)** Standard rift basin. **B)** Type 1 rift basin. **C)** Type 2 rift basin. **D)** Type 3 rift basin. T is motion toward the reader; A is motion away from the reader. The map is displayed at half the size of the cross section. **E)** Type 4 rift basin. See text for discussion.

stages of rifting. Thus, much of the prerift package is preserved beneath the synrift package in these basins. In many rift basins, deformation preceding, and unrelated to, rifting caused uplift and erosion of the prerift strata and the development of a pronounced rift-onset unconformity. For example, at many locations in the Fundy rift basin, the rift-onset unconformity juxtaposes steeply dipping Paleozoic prerift strata with gently dipping Upper Triassic synrift strata (Fig. 16B). Paleozoic orogenic activity, not Mesozoic rifting, produced most of the uplift and erosion associated with this rift-onset unconformity.

The postrift unconformity separates the synrift and postrift packages. When this unconformity develops during the transition from rifting to drifting, it is called the breakup unconformity (e.g., Falvey, 1974). In some rift basins, the postrift unconformity is relatively subtle (e.g., some of the offshore early Mesozoic rift basins of eastern North America) (Fig. 16C). In other rift basins, a pronounced unconformity separates the synrift from the postrift strata (Fig. 16D). Several tectonic processes can produce the uplift and erosion associated with a pronounced postrift unconformity, including: (1) elevation inherited from deformation before rifting (e.g., Schlische, 1990), (2) lateral heat flow from rift centers (e.g., Steckler, 1981), (3) dynamic support by small-scale mantle convection (e.g., Keen, 1985; Steckler, 1985; Buck, 1986), (4) rebound associated with
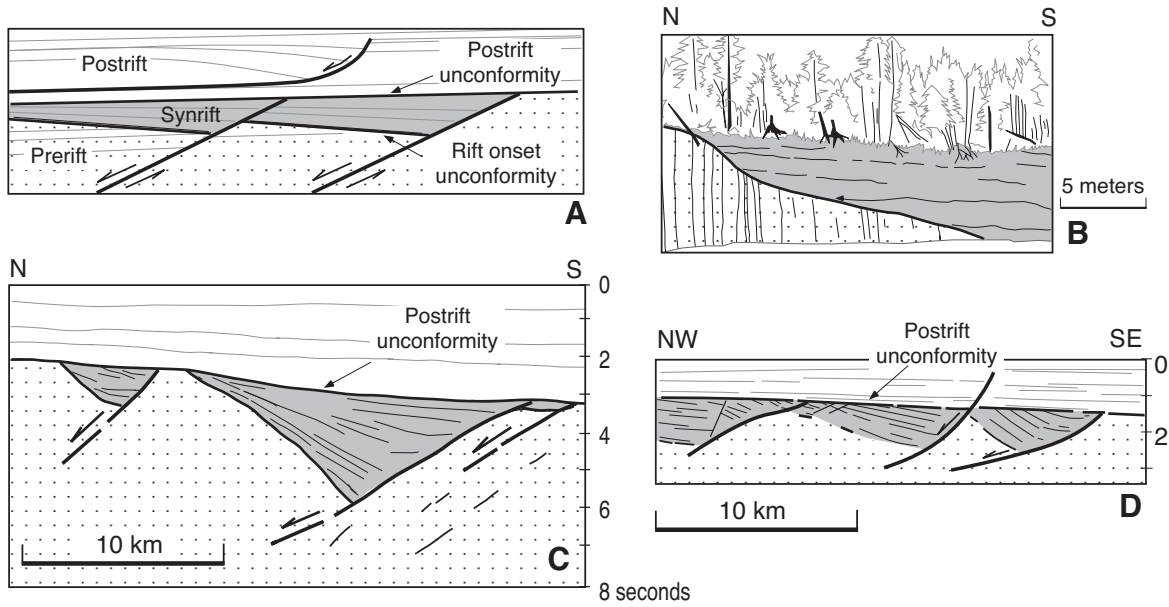
Fig. 16.—**A)** Schematic diagram showing prerift (dotted area), synrift (gray area), and postrift (white area) packages and rift-onset and postrift unconformities. **B)** Field sketch showing a pronounced rift-onset unconformity in the Fundy rift basin (near Tennycape, Nova Scotia) juxtaposing vertical Carboniferous prerift strata with gently dipping Upper Triassic synrift strata (after Schlische and Anders, 1996). **C)** Line drawing of a seismic section from the Atlantis rift basin, offshore eastern North America (after Hutchinson et al., 1986; Schlische and Olsen, 1990). Note the relatively subtle breakup unconformity between the synrift and postrift sections. **D)** Line drawing of a part of seismic line 3630-1/2-85 through the Emerald/Naskapi rift basin of offshore Nova Scotia, one of the offshore Mesozoic rift basins of eastern North America (after Tankard and Welsink, 1989; Withjack et al., 1998). Note the pronounced breakup unconformity between the synrift and postrift sections.

stress relaxation during the rift–drift transition (e.g., Braun and Beaumont, 1989), (5) igneous underplating (Brodie and White, 1994), and/or (6) crustal shortening and inversion after rifting (Withjack et al., 1998).

It is not always possible to definitively identify the prerift, synrift, and postrift units. Rift basins are large-scale features. Without a truly regional perspective (e.g., regional seismic lines rather than local 3D seismic lines), it may not be possible to recognize subtle thickening toward the faulted margin. Thus, the synrift strata may be mistaken for prerift or postrift strata because of a lack of obvious growth beds. Also, faults that detach within salt or shale commonly develop after rifting (Fig. 16A). These detached faults can be mistaken for synrift normal faults and their hanging-wall strata can be mistaken for synrift strata.

Synrift Package

Most rift basins develop in stages (Fig. 17). During the early stages of rifting, numerous isolated normal faults form (e.g., Cowie, 1998; Gupta et al., 1998) (Fig. 17A). As rifting progresses, some of these normal faults lengthen and coalesce while others become inactive (Fig. 17B). During the late stages of rifting, the process of fault linkage produces a border-fault system. The rift basin widens significantly, and the footwalls of the border fault rise. This uplift of the rift flank typically begins several million years after the onset of rifting. For example, detailed fieldwork by Illies (1977) and Garfunkel and Bartov (1977) demonstrated that uplift and erosion of the rift flank began about 10 to 15 million years after rift initiation in the Upper Rhine rift basin and the Suez rift basin, respectively. In many rift basins, an unconformity

separates the early synrift strata from the later synrift strata (e.g., Garfunkel and Bartov, 1977; Olsen, 1997). During the final stages of rifting, new normal faults can develop, dissecting the rift basin. In western Nevada, second and third generations of normal faults formed after the first generation of normal faults rotated to low angles (Proffett, 1977). Apparently, the decrease in fault dip caused the first generation of normal faults to become inactive. New, high-angle normal faults replaced the low-angle normal faults.
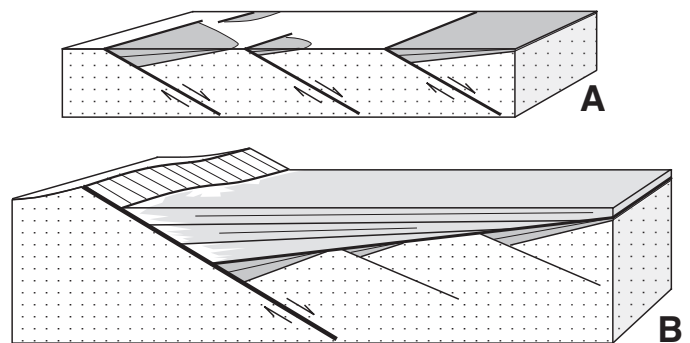

Fig. 17.—Schematic drawings showing the evolution of rift basins. **A)** Early rifting with several minor, relatively isolated normal faults. **B)** Mature rifting with a through-going border-fault system, widespread deposition, footwall uplift, and erosion. The dotted area represents prerift strata and crystalline basement, and the gray areas are synrift strata.

STRUCTURAL CONTROLS ON SEDIMENTARY SYSTEMS

The accommodation space created by faulting and fault-related topography is the primary control on the large-scale sedimentary systems within rift basins. This topic has been addressed in many papers (e.g., Barr, 1987; Leeder and Gawthorpe, 1987; Blair and Bilodeau, 1988; Gibson et al., 1989; Lambiase, 1990; Schlische and Olsen, 1990; Schlische, 1991; Gawthorpe and Hurst, 1993; Lambiase and Bosworth, 1995; Leeder, 1995; Schlische and Anders, 1996; Contreras et al., 1997; Gawthorpe and Leeder, 2000). This section briefly reviews some of the more fundamental structural controls on sedimentary systems and highlights some recent developments.

Depositional Patterns in Transverse Cross Sections

In cross sections perpendicular to the border-fault system, rift basins exhibit a variety of depositional patterns (Fig. 18). In many rift basins, troughs form that deepen toward the border faults. In asymmetric rift basins, the trough forms on one side of the rift basin (Figs. 1A–C), whereas in symmetric rift basins, troughs form on both sides of the rift basin (Fig. 1D). Progressive faulting
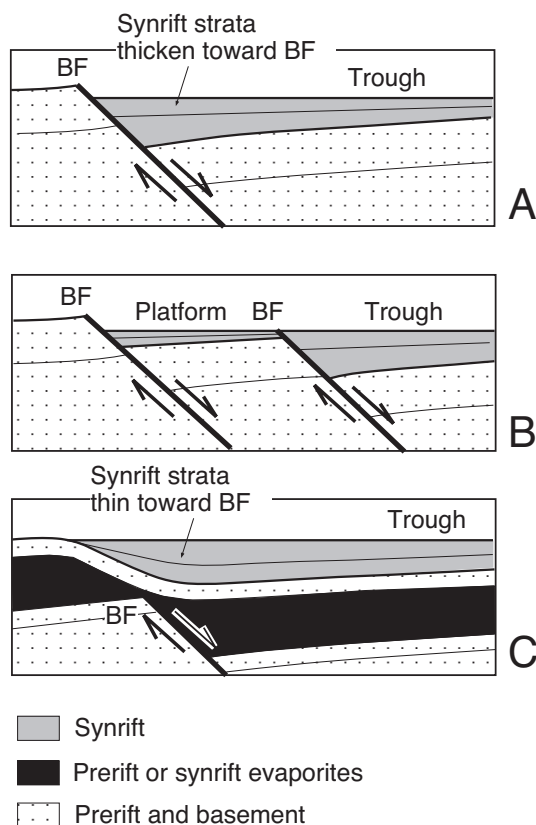

FIG. 18.—Possible geometries of synrift sedimentary units near border faults in transverse cross sections. **A)** Rift basin with a single border fault (BF). Synrift strata thicken toward the border fault. **B)** Rift basin with a platform between parallel, overlapping border faults. Synrift strata on the platform are considerably thinner than equivalent units in the main trough. **C)** Type 1 rift basin with a fault-propagation fold above the border fault. Synrift strata thin, rather than thicken, toward the border fault.

and infilling combine to produce a wedge-shaped unit in which the synrift strata thicken toward the border faults and the younger strata dip less steeply than older strata (Fig. 18A). In many rift basins, platforms develop between parallel, overlapping border faults that dip in the same direction (Figs. 1E–H). These platforms have an intermediate elevation relative to the rift flank and trough and, consequently, contain a much thinner sequence of synrift strata than the trough (Fig. 18B). For example, synrift sedimentary packages on the platforms of the Suez rift basin are generally less than half as thick as coeval packages within the trough (Garfunkel and Bartov, 1977). The platforms contain more unconformities than the trough. In most Type 1 rift basins, extensional forced folds form above the border faults (Figs. 1H, 12E, and 13). In these rift basins, troughs form that deepen away from, rather than toward, the border faults (Fig. 18C). Progressive folding and deposition combine to produce a wedge-shaped sedimentary unit in which the synrift strata thin toward the border faults. Any synrift strata deposited after a border fault has propagated to the surface, however, thicken toward the border fault (e.g, Gawthorpe et al., 1997).

Depositional Patterns in Longitudinal Cross Sections

In cross sections parallel to the border-fault system, most rift basins consist of one or more troughs separated by intrabasin highs (Fig. 4). The troughs form in the hanging walls of the rift-basin border faults. Sedimentary units thin from the centers toward the edges of the troughs (Fig. 5B). The troughs, especially if isolated from each other, can contain very different stratigraphies (e.g., Lambiase and Bosworth, 1995). If the border faults lengthen through time, then the troughs grow longitudinally through time. Longitudinal onlap, reflecting this longitudinal growth, has been observed in some rift basins (Illies, 1977; Schlische, 1991). Some East African rift basins, however, show limited longitudinal onlap (Morley, 1999a). Morley (1999a) concluded that, in these rift basins, the border-fault segments reached a critical length during the early stages of rifting with little additional lengthening during the late stages of rifting.

Intrabasin highs commonly form between stepping border faults with similar dip directions (Fig. 19A). The evolving geometry of the border faults controls whether or not these intrabasin highs persist through time (Anders and Schlische, 1994; Schlische and Anders, 1996). Generally, border faults that become physically connected (hard-linked) produce ephemeral intrabasin highs. Early synrift units are thin to absent in the region of the intrabasin high (Fig. 19A, stage 1), whereas later synrift units do not thin across the former location of the intrabasin high (Fig. 19A, stage 2). If segments do not become hard linked and displacement is partitioned among several overlapping segments, then the intrabasin highs persist throughout synrift sedimentation. Intrabasin highs also form between stepping border faults with convergent dip directions (Fig. 19B). These large-scale transfer zones are commonly areas of reduced subsidence in the Suez rift basin (e.g., Patton et al., 1994; Moustafa, 1996) and in many of the East African rift basins (e.g., Rosendahl, 1987; Morley et al., 1990; Lambiase and Bosworth, 1995). Generally, early synrift units are thin to absent in the transfer zone (Fig. 19B, stage 1). If the overlap of the stepping border faults increases, then the formerly isolated troughs can merge (Fig. 19B, stage 2). The transfer zone, however, remains an area of reduced subsidence.

Influence of Footwall Uplift

The fault-controlled topography surrounding a rift basin also strongly influences sedimentary systems (e.g., Leeder and
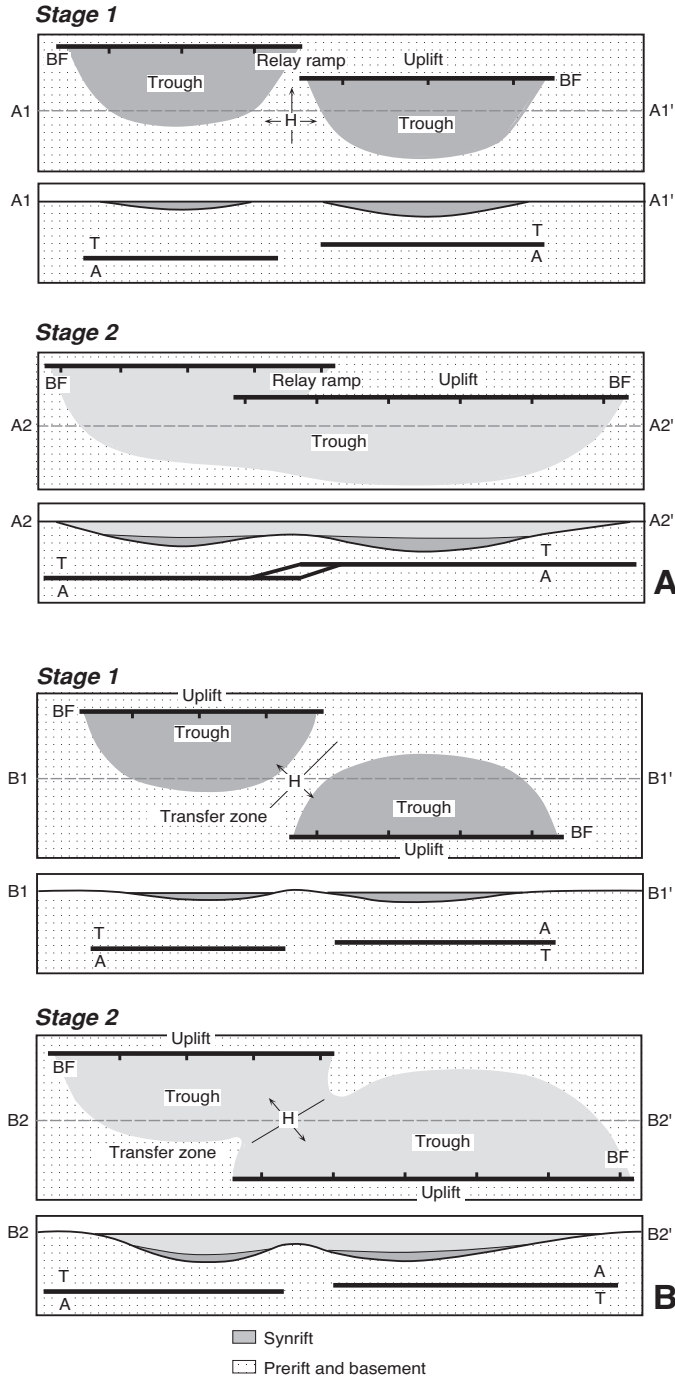
Fig. 19.—Possible geometries of synrift sedimentary units in longitudinal cross sections. Maps (top diagrams in A and B) show the location of cross sections A–A' and B–B', respectively. **A)** Rift basins with stepping border faults (BF) with similar dip directions. **B)** Rift basin with stepping border faults with convergent dip directions shown in two stages. The black line beneath the basin fill in the cross sections is a strike view of the border fault. T is motion toward the reader; A is motion away from the reader. See text for discussion.

Gawthorpe, 1987). Footwall uplift generally produces topographic surfaces that slope away from, and drainages that flow away from, the rift basin. Thus, except for the circumstances listed below, the eroded footwall supplies little sediment directly to the adjacent rift basin. (1) Small drainage systems can exist on the fault-line scarp associated with the border-fault system (Cohen, 1990). These drainage systems can supply limited sediment to the rift basin. (2) Streams can enter the rift basin from the footwall region between border faults where footwall uplift is minimal. This includes relay ramps between stepping border faults with similar dip directions (e.g., Gawthorpe and Hurst, 1993; Childs et al., 1995; Lambiase and Bosworth, 1995). In the Newark rift basin, conglomeratic alluvial-fan facies along the border-fault system are preferentially associated with such relay ramps (e.g., Schlische, 1992). Streams may also enter at transfer zones associated with stepping border faults with convergent dip directions (e.g., Morley et al., 1990; Childs et al., 1995; Lambiase and Bosworth, 1995). (3) Streams can flow across the footwall block if large antecedent drainages are able to erode through the uplifting footwall blocks. For example, in the Connecticut Valley rift basin in eastern North America, streams entered the basin from the footwall when fault-displacement rates were low and from the hanging wall when displacement rates were higher (e.g., Olsen, 1997). The topography on the hinged margin, if present, slopes toward the rift basin, and many streams enter the basin along this route (e.g., Leeder and Gawthorpe, 1987; Cohen, 1990). Many streams also enter a rift basin axially (e.g., Cohen, 1990; Lambiase, 1990; Lambiase and Bosworth, 1995), including streams that flow around the footwall uplift.

Influence of Intrabasin Faults and Folds

Intrabasin faults and folds also influence the depositional patterns of rift basins. Fault-displacement folds locally influence sedimentation, with synrift units thickening in the synclinal lows and thinning on the anticlinal highs in the footwalls and hanging walls of intrabasin normal faults (e.g., Figs. 11A and 11C). Schlische (1995) described examples from the Newark rift basin in eastern North America, and Dawers and Underhill (2000) and McLeod et al. (2000) described examples from the depocenter adjacent to the Statfjord fault in the Viking rift basin of the northern North Sea. Fault-propagation folding and forced folding also locally affect depositional patterns. For example, fault-propagation folding has influenced depositional patterns in the Suez rift basin (Gawthorpe et al., 1997; Gupta et al., 1999; Sharp et al., 2000) and in the Haltenbanken area of the Vøring rift basin (e.g., Figs. 13C and 13D). Progressive folding and deposition combine to produce a wedge-shaped sedimentary unit in which the synrift strata thin toward the underlying intrabasin faults.

Depositional Environments of Nonmarine Rift Basins

A wide variety of depositional environments are present in nonmarine rift basins, but two depositional regimes predominate: fluvial and lacustrine. Fluvial depositional systems require a slope, whereas lacustrine (ponded water) depositional systems require that the basin outlet be perched above the depositional surface. The relationships among incremental accommodation space (the amount of accommodation space added to a basin for a given time increment), sediment supply, and water supply determine which depositional system predominates in a given rift basin (Schlische and Olsen, 1990; Schlische, 1991; Schlische and Anders, 1996; Olsen, 1997; Carroll and Bohacs, 1999) (Fig. 20). In cases where the sediment supply exceeds the incremental accommodation space, fluvial deposition predominates (Fig. 20A).
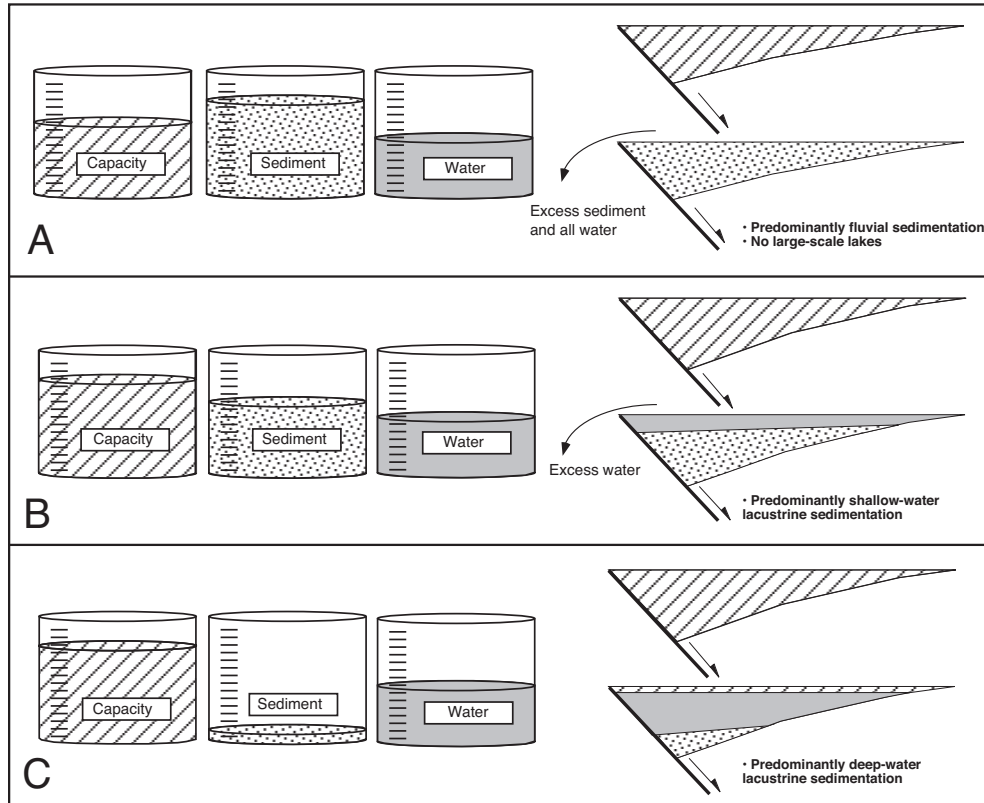
FIG. 20.—Relationships among basin capacity (incremental accommodation space), sediment supply, and water supply in nonmarine rift basins. **A)** Sediment supply exceeds basin capacity. **B)** Basin capacity exceeds sediment supply and water supply exceeds excess basin capacity. **C)** Basin capacity greatly exceeds sediment supply and water supply is less than excess basin capacity. See text for discussion.

In cases where the incremental accommodation space exceeds the sediment supply, lacustrine deposition predominates (although deltaic and fluvial deposition occurs around the margins of the lake). The relationship between the available supply of water and the excess capacity (the difference between the incremental accommodation space and the sediment supply) of the basin determines the hydrological conditions in the lake. If the water supply exceeds the excess capacity, the lake is hydrologically open (Fig. 20B). If the excess capacity exceeds the water supply, the lake is hydrologically closed (Fig. 20C). Given these relationships, the depth of the lake is an unreliable recorder of climate. For example, if the excess capacity of the basin is very small, the lake depth is controlled by the distance between the depositional surface and the lowest outlet. Thus, even if the climate is very wet, the lake will still be shallow.

Many nonmarine rift basins from a wide variety of climatic regimes and tectonic settings share a similar synrift stratigraphic architecture (e.g., Lambiase, 1990; Schlische and Olsen, 1990). The succession generally begins with a fluvial unit. This is overlain by a lacustrine unit that demonstrates a rapid deepening-upward interval to a lake-highstand interval. The deep-water lacustrine interval is succeeded by a gradually upward-shoaling lacustrine unit that is commonly capped by a fluvial unit. This succession is known as a tripartite stratigraphy. Lambiase (1990) observed that some continental rift basins contain multiple stratigraphic successions, consisting of all or part of the tripartite stratigraphy. For the Mesozoic rift basins of eastern North America, the individual

stratigraphic successions are bounded by unconformities, particularly along the margins of the basins, separating the synrift deposits into tectonostratigraphic packages (Olsen, 1997; Olsen et al., 2000). Some dominantly marine rift basins (e.g., in Crete; Postma and Drinia, 1993) display similar stratigraphic successions. In these cases, marine deposits take the place of lacustrine deposits, but the water depth varies in a manner similar to that of continental rift basins.

Given the relationships among incremental accommodation space, sediment supply, and water supply, several mechanisms can produce the major stratigraphic transitions within the tripartite succession. The fluvial–lacustrine transition may result from an increase in incremental accommodation space and/or a decrease in sediment supply. The shallow-water to deep-water lacustrine transition may result from an increase in incremental accommodation space, a decrease in the sediment supply, or an increase in the water supply. The deep-water to shallow-water lacustrine transition may result from a decrease or increase in incremental accommodation space (depending on the geometry of the excess accommodation space in the basin), an increase in the sediment supply, and/or a decrease in the water supply. The lacustrine–fluvial transition may result from a decrease in incremental accommodation space or an increase in sediment supply. Because three of four of the stratigraphic transitions may result from an increase in incremental accommodation space and because accommodation space is structurally controlled (e.g., Leeder and Gawthorpe, 1987; Gibson et al., 1989), the structural evolu-

tion of rift basins most strongly influences the stratigraphic architecture (Lambiase, 1990; Schlische and Olsen, 1990; Schlische, 1991; Contreras et al., 1997).

Basin-Filling Models for Rift Basins

The basin-filling model of Schlische (1991) emphasized the role of fault growth in an asymmetric rift basin with a single border fault (Fig. 21). As discussed previously, faults generally increase in length as fault displacement increases. Thus, as displacement on the border fault accrues, the rift basin generally increases in depth, length, and width. Thus, incremental accommodation space within the basin increases through time. If sedimentation keeps pace with incremental accommodation space, then the basin is always filled to its lowest outlet with sediment. Strata progressively onlap the hanging-wall hinged margin as the basin widens and lengthens through time. It is unlikely, however, that sedimentation always keeps pace with incremental accommodation space. If the sediment-supply rate and the water-supply rate are constant and if the incremental accommodation space progressively increases, then the rift basin undergoes three of the four major stratigraphic transitions contained within the tripartite stratigraphy. The fourth major stratigraphic transition, the lacustrine–fluvial transition, cannot be reproduced in a basin-filling model that requires a progressive increase in incremental accommodation space. Accommodation space, however, cannot increase indefinitely. Once extension slows considerably or ceases, the basin gradually infills with sediment, with fluvial conditions returning when sediment supply exceeds incremental accommodation space. Multiple extensional pulses may produce multiple synrift tectonostratigraphic packages separated by unconformities if the time between pulses is large (Olsen, 1997).

The quantitative basin-filling models of Contreras et al. (1997) predicted how accumulation rates vary with location and through time. These predictions are in broad agreement with actual accumulation rates from the Newark rift basin (Olsen, 1997). The qualitative basin-filling models of Lambiase (1990) and Lambiase and Bosworth (1995) emphasized the role of footwall uplift and transfer zones. They argued that deep lakes form only when high relief is produced by significant footwall uplift and the formation of transfer zones between stepping borders faults with convergent dip directions. They also pointed out that depocenters bounded by transfer zones exhibit different stratigraphies, particularly if a large axial supply of sediment exists. In this case, the depocenter located nearest the axial supply is the first to become completely infilled, with succeeding depocenters in the sediment-transport direction being progressively infilled. Smoot (1991) presented a qualitative basin-filling model that is most appropriate for the initial fluvial deposits and immediately succeeding lacustrine deposits. He hypothesized that reductions in fluvial gradients and clogging of the basin's outlets contribute to the fluvial–lacustrine transition. This model accounts for a change from initial braided-stream deposits to meandering-stream deposits observed in the basal fluvial sequences of many Mesozoic rift basins in eastern North America.

Gupta et al. (1998) and Cowie et al. (2000) presented a semiquantitative model to explain the large-scale structural and stratigraphic evolution of rift basins. They noted that many marine rift basins appear to undergo a period of accelerated subsidence (associated with deeper-water marine sedimentation) several million years after the initiation of rifting. Their basin-evolution model, based on the results of numerical models of fault-population evolution, showed that certain normal faults undergo periods of accelerated displacement, even though the regional extensional strain rate is constant (Cowie et al., 1995;

Cowie, 1998; Cowie et al., 2000). They proposed that the period of increased subsidence and deeper-water marine sedimentation observed in many marine rift basins correlates with the period of strain localization on faults within the border-fault system. Applying their model to nonmarine rift basins, the period of widely distributed faulting would correspond to fluvial sedimentation, whereas deep-water lacustrine sedimentation would correspond to the phase of strain localization.

Influence of Plate-Tectonic Movements on Sedimentary Systems

The forgoing discussion has highlighted how the structure within rift basins and rift systems influences sedimentary systems. Tectonics at the plate-tectonic scale also influences sedimentary systems. Plate movement can cause a rift basin to drift from one climatic zone to another. For example, the Mesozoic rift basins of eastern North America gradually drifted northward during Late Triassic and Early Jurassic time (e.g., Olsen et al., 2000; Olsen, 1997; Olsen and Kent, 2000). Relatively humid facies were deposited when a basin was located near the paleoequator, whereas relatively arid facies were deposited when a basin was located at more northern latitudes. Given the structural control on the tripartite stratigraphic architecture of synrift strata discussed above, it is important to draw a distinction between humid and arid facies deposited under different climatic regimes versus fluvial and lacustrine strata deposited under different hydrologic conditions (Olsen et al., 2000). The combinations of various facies (e.g., arid fluvial, humid fluvial, arid lacustrine, humid lacustrine) are produced by the creation of accommodation space by border faults, the balance between accommodation space and sediment infilling, and changes in climatic regime controlled by the drift of tectonic plates.

SUMMARY

1. Rift basins are complex features defined by several large-scale structural components including faulted margins, the border faults of the faulted margins, the uplifted flanks of the faulted margins, hinged margins, deep troughs, large-scale intrabasin fault blocks, and large-scale transfer zones. A variety of moderate- to small-scale structures also develop within rift basins. These structures include normal faults (basement-involved and detached), strike-slip and reverse faults, and extensional folds (fault-displacement, fault-propagation, forced, and fault-bend). All of these structures, regardless of their size, affect the depositional patterns of rift basins by creating sites of uplift and erosion, by influencing pathways of sediment transport, and by defining the accommodation space for sediment deposition and preservation.

2. To provide a framework for understanding the variety of structural styles in rift basins, we have defined a standard rift basin and four end-member variations. Most rift basins have attributes of the standard rift basin and one or more of the end-member variations. The standard rift basin has little salt or shale in the prerift or synrift packages. Few preexisting zones of weakness in the prerift strata or crystalline basement were reactivated during rifting, and little tectonic activity followed rifting. The standard rift basin is characterized by moderately to steeply dipping basement-involved normal faults that strike roughly perpendicular to the direction of maximum extension. Type 1 rift basins have salt or thick shale in the prerift or synrift packages. They are characterized by extensional forced folds above basement-in-

volved normal faults and detached normal faults with associated fault-bend folds. Contractional activity preceded rifting in Type 2 rift basins. Many of the normal faults in these rift basins are thrust faults reactivated with normal displacement and, thus, are low-angle. Type 3 rift basins are produced by oblique rifting. They are characterized by faults with strike-slip, normal, and oblique-slip displacement that are parallel and oblique to the rift trend. One or more contractional events followed rifting in Type 4 rift basins. These inverted rift basins are affected by late-formed contractional structures including normal faults reactivated as

reverse faults, newly formed reverse faults, and contractional fault-bend and fault-propagation folds.

3. Most rift basins are composed of several troughs separated by intrabasin highs. The arrangement of the troughs and highs depends on the arrangement of the rift-basin border faults. If the border faults are stepping and have similar dip directions, then a series of adjacent troughs and highs develops on the faulted margin of the rift basin. These intrabasin highs are commonly ephemeral because the stepping border faults become hard linked. If the border faults are stepping and have

Stage 1

Capacity < sediment supply

Fluvial sedimentation

Stage 2

Capacity = sediment supply

Fluvial-lacustrine transition

Stage 3

Capacity > sediment supply

Water volume > excess capacity

Shallow-water lacustrine sedimentation

Stage 4

Capacity >> sediment supply

Water volume = excess capacity

Deep-water lacustrine sedimentation

Stage 5

Capacity > sediment supply

Water volume < excess capacity
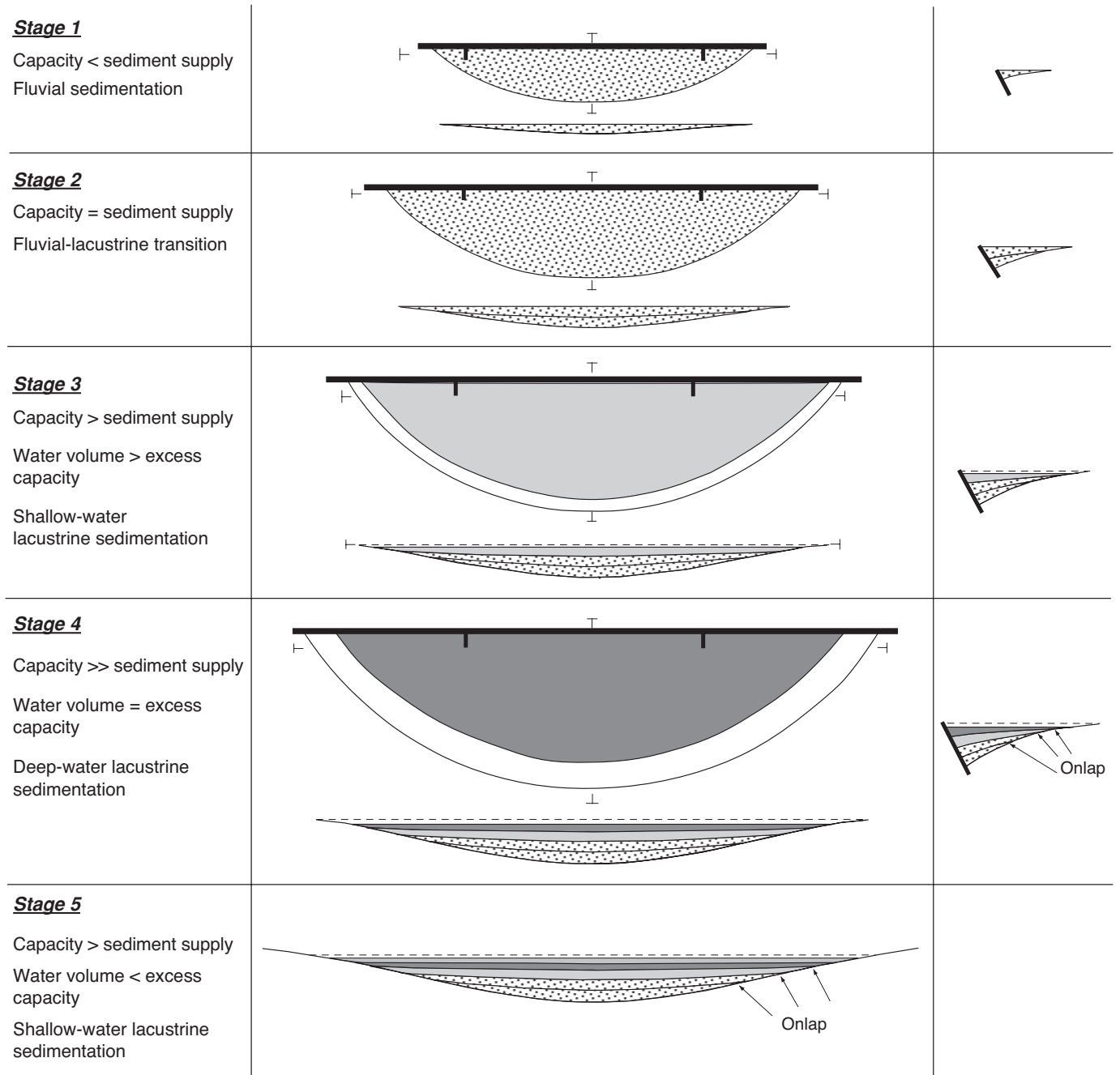
Shallow-water lacustrine sedimentation

Fig. 21.—Simple filling model for a growing asymmetric rift basin shown in map view (stages 1–4), longitudinal cross section (stages 1–5), and transverse cross sections (stages 1–4). Dashed lines represent lake level. Modified from Schlische and Anders (1996).

convergent dip directions, then a series of offset troughs separated by highs develops on opposing sides of the rift basin. Generally, synrift units are thin to absent on these intrabasin highs throughout synrift sedimentation.

4. In cross sections perpendicular to the border-fault system, rift basins exhibit a variety of structural and depositional patterns. In many rift basins, troughs form that deepen toward the border faults. Progressive faulting and infilling combine to produce a wedge-shaped unit in which the synrift strata thicken toward the border faults. In other rift basins, platforms develop between parallel, overlapping border faults that dip in the same direction. These platforms have an intermediate elevation relative to the rift flank and trough and, consequently, contain a much thinner sequence of synrift strata than the trough. In most Type 1 rift basins, an extensional forced fold forms above the border faults. In these rift basins, troughs form that deepen away from, rather than toward, the border faults. Progressive folding and deposition combine to produce a wedge-shaped sedimentary unit in which the synrift strata thin toward the border faults.

5. Many nonmarine rift basins share a similar synrift stratigraphic architecture known as a tripartite stratigraphy. The succession begins with a fluvial unit. This is overlain by a lacustrine unit that demonstrates a rapid deepening-upward interval to a lake-highstand interval. This is succeeded by a gradually upward-shoaling lacustrine unit that is commonly capped by a fluvial unit. These stratigraphic transitions result from changes in the relative balance between sediment supply, water supply, and accommodation space, the last of which is structurally controlled. Fluvial sedimentation occurs when sediment supply exceeds accommodation space. Lacustrine sedimentation results when accommodation space exceeds sediment supply. Hydrologically open lakes result when the supply of water exceeds the basin's excess capacity (accommodation space minus sediment supply). Hydrologically closed lakes result when the supply of water is less than the excess capacity.

6. A simple rift basin increases in depth, length, and width as displacement on its border-fault system accrues. Thus, incremental accommodation space increases through time. If sedimentation keeps pace with incremental accommodation space, then the basin is always filled to its lowest outlet with sediment. If the sediment-supply rate and the water-supply rate are constant and if the incremental accommodation space progressively increases, then the rift basin may undergo three of the four major stratigraphic transitions contained within the tripartite stratigraphy. The final lacustrine-fluvial transition requires that faulting slow considerably or cease. As a result, the basin gradually infills with sediment, with fluvial conditions returning when sediment supply exceeds incremental accommodation space.

ACKNOWLEDGMENTS

REFERENCES

ACKERMANN, R.V., SCHLISCHE, R.W., AND WITHJACK, M.O., 2001, The geometric and statistical evolution of normal fault systems: an experimental study of the effects of mechanical layer thickness on scaling laws: Journal of Structural Geology, v. 23, p. 1803–1819.

ANDERS, M.H., AND SCHLISCHE, R.W., 1994, Overlapping faults, intrabasin highs, and the growth of normal faults: Journal of Geology, v. 102, p. 165–179.

ANGELIER, J., AND BERGERAT, F., 1983, Systemés de contrainte et extension intracontinentale: Bull. Centres Recherches Exploration–Production Elf-Aquitaine, v. 7, p. 137–147.

BAKER, B.H., AND WOHLENBERG, J., 1971, Structure and evolution of the Kenya rift valley: Nature, v. 229, p. 538–542.

BARNETT, J.A.M., MORTIMER, J., RIPPON, J.H., WALSH, J.J., AND WATTERSON, J., 1987, Displacement geometry in the volume containing a single normal fault: American Association of Petroleum Geologists, Bulletin, v. 71, p. 925–937.

BARR, D., 1987, Structural/stratigraphic models for extensional basins of half-graben type: Journal of Structural Geology, v. 9, p. 491–500.

BLAIR, T.C., AND BILODEAU, W.L., 1988, Development of tectonic cyclothems in rift, pull-apart, and foreland basins—sedimentary response to episodic tectonism: Geology, v. 16, p. 517–520.

BLYSTAD, P., BREKKE, H., FAERSETH, R.B., LARSEN, B.T., SKOGSEID, J., AND TØRUDBAKKEN, B., 1995, Structural Elements of the Norwegian Continental Shelf, Part II—The Norwegian Sea Region: Norwegian Petroleum Directorate, Bulletin 8, 45 p.

BRAUN, J., AND BEAUMONT, C., 1989, A physical explanation of the relation between flank uplifts and the breakup unconformity at rifted continental margins: Geology, v. 17, p. 760–764.

BREYER, F., 1974, Structure and development of the southern part of the Rhine graben according to geological and geophysical observations, *in* Illies, J.H., and Fuchs, K., eds., Approaches to Taphrogenesis: Inter-Union Commission on Geodynamics, Scientific Report 8, p. 145–155.

BRODIE, J., AND WHITE, N.J., 1994, Sedimentary basin inversion caused by igneous underplating: Northwest European continental shelf: Geology, v. 22, p. 147–150.

BROWN, R.N., 1980, History of exploration and discovery of Morgan, Ramadan, and July oilfields, Gulf of Suez, Egypt, *in* Maill, A.D., ed., Facts and Principles of World Petroleum Occurrence: Canadian Society of Petroleum Geologists, Memoir 6, p. 733–764.

BUCK, W.R., 1986, Small-scale convection induced by passive rifting—the cause for uplift of rift shoulders: Earth and Planetary Science Letters, v. 77, p. 362–372.

CARROLL, A.R., AND BOHACS, K.M., 1999, Stratigraphic classification of ancient lakes—balancing tectonic and climatic controls: Geology, v. 27, p. 99–102.

CHAMBERLIN, R.N., 1983, Cenozoic domino-style crustal extension in the Lemitar Mountains, New Mexico: a summary: New Mexico Geological Society 34th Field Conference, Guidebook, Socorro Region II, p. 111–118.

CHAPMAN, G.R., LIPPARD, S.J., AND MARTYN, J.E., 1978, The stratigraphy and structure of the Kamasia Range, Kenya Rift Valley: Geological Society of London, Journal, v. 135, p. 265–281.

CHILDS, C., WATTERSON, J., AND WALSH, J.J., 1995, Fault overlap zones within developing normal fault systems: Geological Society of London, Journal, v. 152, p. 535–549.

CLIFTON, A.E., SCHLISCHE, R.W., WITHJACK, M.O., AND ACKERMANN, R.V., 2000, Influence of rift obliquity on fault-population systematics: results of clay modeling experiments: Journal of Structural Geology, v. 22, p. 1491–1509.

COFFIELD, D.Q., AND SCHAMEL, S., 1989, Surface expression of an accommodation zone within the Gulf of Suez rift, Egypt: Geology, v. 17, p. 76–79.

COHEN, A.S., 1990, Tectono-stratigraphic model for sedimentation in Lake Tanganyika, Africa, *in* Katz, B.J., ed., Lacustrine Basin Exploration—

Case Studies and Modern Analogs: American Association of Petroleum Geologists, Memoir 50, p. 137–150.

COLLETTA, B., LE QUELLEC, P., LETOUZEY, J., AND MORETTI, I., 1988, Longitudinal evolution of the Suez structure (Egypt): Tectonophysics, v. 153, p. 221–233.

CONTINI, D., AND THEOBALD, N., 1974, Relations entre le Fosse Rhenan et le Fosse de la Soane, tectonique des régions sous-vosgiennes et préjurassiennes, *in* Illies, J.H. and Fuchs, K., eds., Approaches to Taphrogenesis: Inter-Union Commission on Geodynamics, Scientific Report 8, p. 310–321.

CONTRERAS, J., SCHOLZ, C.H., AND KING, G.C.P., 1997, A general model of rift basin evolution: constraints of first order stratigraphic observations: Journal of Geophysical Research, v. 102, p. 7673–7690.

COOPER, M.A., AND WILLIAMS, G.D., eds., 1989, Inversion Tectonics: Geological Society of London, Special Publication 44, 375 p.

COWIE, P.A., 1998, A healing–reloading feedback control on the growth rate of seismogenic faults: Journal of Structural Geology, v. 20, p. 1075–1088.

COWIE, P.A., GUPTA, S., AND DAWERS, N.H., 2000, Implications of fault array evolution for synrift depocentre development: insights from a numerical fault growth model: Basin Research, v. 12, p. 241–261.

COWIE, P.A., SORNETTE, D., AND VANNESTE, C., 1995, Multifractal scaling properties of a growing fault population: Geophysical Journal International, v. 122, p. 457–469.

DAVISON, I., 1987, Normal fault geometry related to sediment compaction and burial: Journal of Structural Geology, v. 9, p. 393–401.

DAWERS, N.H., ANDERS, M.H., AND SCHOLZ, C.H., 1993, Growth of normal faults—displacement-length scaling: Geology, v. 21, p. 1107–1110.

DAWERS, N.H., AND UNDERHILL, J.R., 2000, The role of fault interaction and linkage in controlling synrift stratigraphic sequences—Late Jurassic, Statfjord East area, northern North Sea: American Association of Petroleum Geologists, Bulletin, v. 84, p. 45–64.

DE VOOGD, B., KEEN, C.E., AND KAY, W.A., 1990, Fault reactivation during Mesozoic extension in eastern offshore Canada: Tectonophysics, v. 173, p. 567–580.

EBINGER, C.J., ROSENDAHL, B.R., AND REYNOLDS, D.J., 1987, Tectonic model of the Malawi rift, Africa: Tectonophysics, v. 141, p. 215–235.

FALVEY, D.A., 1974, The development of continental margins in plate tectonic theory: APEA Journal, v. 14, p. 95–106.

FAULDS, J.E., AND VARGA, R.J., 1998, The role of accommodation zones and transfer zones in the regional segmentation of extended terranes, *in* Faulds, J.E., and Stewart, J.H., eds., Accommodation Zones and Transfer Zones: The Regional Segmentation of the Basin and Range Province: Geological Society of America, Special Paper 323, p. 1–45.

GARFUNKEL, Z., AND BARTOV, Y., 1977, The tectonics of the Suez rift: Geological Survey of Israel, Bulletin 71, 44 p.

GAWARECKI, S.L., AND COFFIELD, D.Q., 1990, Mechanical response to stratigraphic inhomogeneity during extension, and surface expression of buried structures, Gulf of Suez, Egypt: Tectonophysics, v. 174, p.7–20.

GAWTHORPE, R.L., AND HURST, J.M., 1993, Transfer zones in extensional basins—their structural style and influence on drainage development and stratigraphy: Geological Society of London, Journal, v. 150, p. 1137–1152.

GAWTHORPE, R.L., AND LEEDER, M.R., 2000, Tectono-sedimentary evolution of active extensional basins: Basin Research, v. 12, p. 195–218.

GAWTHORPE, R.L., SHARP, I., UNDERHILL, J.R., AND GUPTA, S., 1997, Linked sequence stratigraphic and structural evolution of propagating normal faults: Geology, v. 25, p. 795–798.

GIBSON, J.R., WALSH, J.J., AND WATTERSON, J., 1989, Modelling of bed contours and cross-sections adjacent to planar normal faults: Journal of Structural Geology, v. 11, p. 317–328.

GOGUEL, J., 1962, Tectonics (translated from French edition, 1952, by Thalman, H.E.): San Francisco, Freeman, 384 p.

GUPTA, S., COWIE, P.A., DAWERS, N.H., AND UNDERHILL, J.R., 1998, A mechanism to explain rift-basin subsidence and stratigraphic patterns through fault-array evolution: Geology, v. 26, p. 595–598.

GUPTA, S., UNDERHILL, J.R., SHARP, I.R., AND GAWTHORPE, R.L., 1999, Role of fault interactions in controlling synrift sediment dispersal patterns—Miocene, Abu Alaqa Group, Suez rift, Sinai, Egypt: Basin Research, v. 11, p. 167–189.

HAMBLIN, W.K., 1965, Origin of "reverse drag" on the downthrown sides of normal faults: Geological Society of America, Bulletin, v. 76, p. 1145–1164.

HORSFIELD, W.T., 1977, An experimental approach to basement-controlled faulting: Geologie en Mijnbouw, v. 56, p. 363–370.

HUTCHINSON, D.R., KLITGORD, K.D., AND DETRICK, R.S., 1986, Rift basins of the Long Island Platform: Geological Society of America, Bulletin, v. 97, p. 688–702.

ILLIES, J.H., 1977, Ancient and recent rifting in the Rhinegraben: Geologie en Mijnbouw, v. 56, p. 329–350.

ILLIES, J.H., AND GREINER, G., 1978, Rhinegraben and Alpine system: Geological Society of America, Bulletin, v. 89, p. 770–782.

JACKSON, J., AND LEEDER, M., 1994, Drainage systems and the development of normal faults—an example from Pleasant Valley, Nevada: Journal of Structural Geology, v. 16, p. 1041–1059.

JACKSON, J., AND MCKENZIE, D., 1983, The geometrical evolution of normal fault systems: Journal of Structural Geology, v. 5, p. 471–482.

JANECKE, S.U., VANDERBURG, C.J., AND BLANKENAU, J.J., 1998, Geometry, mechanisms and significance of extensional folds from examples in the Rocky Mountain Basin and Range province, U.S.A.: Journal of Structural Geology, v. 20, p. 841–856.

KEEN, C.E., l985, The dynamics of rifting: deformation of the lithosphere by active and passive driving mechanisms: Geophysical Journal of the Royal Astronomical Society, v. 80, p. 95–120.

KEEN, C.E., BOUTILIER, R., DEVOOGD, B., MUDFORD, B., AND ENACHESCU, M.E., 1987, Crustal geometry and extensional models for the Grand Banks, eastern Canada: constraints from deep seismic reflection data, *in* Beaumont, C., and Tankard, A., eds., Sedimentary Basins and Basin-Forming Mechanisms: Canadian Society of Petroleum Geologists, Memoir 12, p. 101–115.

KELLEY, V., 1979, Tectonics, middle Rio Grande rift, New Mexico, *in* Riecker, R.E., ed., Rio Grande Rift: Tectonics and Magmatism: Washington, D.C., American Geophysical Union, p. 57–70.

KING, G., AND ELLIS, M., 1990, The origin of large local uplift in extensional regions: Nature, v. 348, p. 689–693.

LAMBIASE, J.J., 1990, A model for tectonic control of lacustrine stratigraphic sequences in continental rift basins, *in* Katz, B.J., ed., Lacustrine Basin Exploration—Case Studies and Modern Analogs: American Association of Petroleum Geologists, Memoir 50, p. 265–276.

LAMBIASE, J.J., AND BOSWORTH, W., 1995, Structural controls on sedimentation in continental rifts, *in* Lambiase, J.J., ed., Hydrocarbon Habitat in Rift Basins: Geological Society of London, Special Publication 80, p. 117–144.

LARSEN, P.-H., 1988, Relay structures in a Lower Permian basement-involved extension system, East Greenland: Journal of Structural Geology, v. 10, p. 3–8.

LAUBSCHER, H.P., 1982, Die Südostecke des Rheingrabens—ein kinematisches und dynamisches Problem: Eclogae Geologicae Helvetiae, v. 75, p. 101–116.

LEEDER, M.R., 1995, Continental rifts and proto-oceanic rift troughs, *in* Busby, C.J. and Ingersoll, R.V., eds., Tectonics of Sedimentary Basins: Cambridge, Massachusetts, Blackwell, p. 119–148.

LEEDER, M.R., AND GAWTHORPE, R.L., 1987, Sedimentary models for extensional tilt-block/half-graben basins, *in* Coward, M.P., Dewey, J.F., and Hancock, P.L., eds., Continental Extensional Tectonics: Geological Society of London, Special Publication 28, p. 139–152.

LETOUZEY, J., 1990, Fault reactivation, inversion, and fold-thrust belt, *in* Letouzey, J., ed., Petroleum and Tectonics in Mobile Belts: Paris, IFP Editions Technip, p. 101–128

MARCHAL, D., GUIRAUD, M., RIVES, T., AND VAN DEN DRIESSCHE, J., 1998, Space and time propagation processes of normal faults, *in* Jones, G., Fisher, Q.J., and Knipe, R.J., eds., Faulting, Fault Sealing, and Fluid Flow in

Hydrocarbon Reservoirs: Geological Society of London, Special Publication 147, p. 51–70.

MAURIN, J.-C., 1995, Drapage et décollement des séries jurassiques sur la faille de détachement majeure du rift rhénan sud: implications sur la géométrie des dépôts syn-rifts oligocenes: Académie des Sciences [Paris], Comptes Rendus, v. 321, p. 1025–1032.

McLEOD, A.E., DAWERS, N.H., AND UNDERHILL, J.R., 2000, The propagation and linkage of normal faults—Insights from the Strathsey–Brent–Statfjord fault array, northern North Sea: Basin Research, v. 12, p. 263–284.

MORLEY, C.K., 1995, Developments in the structural geology of rifts over the last decade and their impact on hydrocarbon exploration, *in* Lambiase, J.J., ed., Hydrocarbon Habitat in Rift Basins: Geological Society of London, Special Publication 80, p. 1–32.

MORLEY, C.K., 1999a, Patterns of displacement along large normal faults—implications for basin evolution and fault propagation, based on examples from East Africa: American Association of Petroleum Geologists, Bulletin, v. 83, p. 613–634.

MORLEY, C.K., ED. 1999b, Geoscience of Rift Systems—Evolution of East Africa: American Association of Petroleum Geologists, Studies in Geology 44, 250 p.

MORLEY, C.K., NELSON, R.A., PATTON, T.L., AND MUNN, S.G., 1990, Transfer zones in the East African rift system and their relevance to hydrocarbon exploration in rifts: American Association of Petroleum Geologists, Bulletin, v. 74, p. 1234–1253.

MOUSTAFA, A.M., 1976, Block faulting in the Gulf of Suez: Proceedings of the 5th Exploration Seminar, Egyptian General Petroleum Organization, Cairo.

MOUSTAFA, A.R., 1996, Internal structure and deformation of an accommodation zone in the northern part of the Suez rift: Journal of Structural Geology, v. 18, p. 93–108.

MOUSTAFA, A.R., 1997, Controls on the development and evolution of transfer zones—the influence of basement structure and sedimentary thickness in the Suez rift and Red Sea: Journal of Structural Geology, v. 19, p. 755–768.

NELSON, R.A., PATTON, T.L., AND MORLEY, C.K., 1992, Rift-segment interaction and its relation to hydrocarbon exploration in continental rift systems: American Association of Petroleum Geologists, Bulletin, v. 76, p. 1153–1169.

OLSEN, P.E., 1997, Stratigraphic record of the early Mesozoic breakup of Pangea in the Laurasia–Gondwana rift system: Annual Review of Earth and Planetary Sciences, v. 25, p. 337–401.

OLSEN, P.E. AND KENT, D.V., 2000, High resolution early Mesozoic Pangean climatic transect in lacustrine environments, *in* Bachmann, G., and Lerche, I., eds., Epicontinental Triassic, Volume 3, Zentralblatt für Geologie und Paläontologie, VIII, p. 1475–1496.

OLSEN, P.E., KENT, D.V., FOWELL, S.J., SCHLISCHE, R.W., WITHJACK, M.O., AND LETOURNEAU, P.M., 2000, Implications of a comparison of the stratigraphy and depositional environments of the Argana (Morocco) and Fundy (Nova Scotia, Canada) Permian–Jurassic basins, *in* Oujidi, M. and Et-Touhami, M., eds., Le Permien et le Trias du Maroc, Actes de la Premièr Réunion su Groupe Marocain du Permien et du Trias: Oujda, Hilal Impression, p. 165–183.

PATTON, T., 1984, Normal fault and fold development in sedimentary rocks above a pre-existing basement normal fault [unpublished Ph.D. thesis]: Texas A&M University, College Station, 164 p.

PATTON, T.L., MOUSTAFA, A.R., NELSON, R.A., AND ABDINE, S.A., 1994, Tectonic evolution and structural setting of the Suez rift, *in* Landon, S.M., ed., Interior Rift Basins: American Association of Petroleum Geologists, Memoir 59, p. 9–55.

PEACOCK, D.C.P., AND SANDERSON, D.J., 1991, Displacements, segment linkage and relay ramps in normal fault zones: Journal of Structural Geology, v. 13, p. 721–733.

PEACOCK, D.C.P., AND SANDERSON, D.J., 1994, Geometry and development of relay ramps in normal fault systems: American Association of Petroleum Geologists, Bulletin, v. 78, p. 147–165.

PEACOCK, D.C.P., KNIPE, R.J., AND SANDERSON, D.J., 2000, Glossary of normal faults: Journal of Structural Geology, v. 22, p. 291–306.

PLINT, A.G., AND VAN DE POLL, H.W., 1984, Structural and sedimentary history of the Quaco Head area, southern New Brunswick: Canadian Journal of Earth Sciences, v. 21, p. 753–761.

POSTMA, G., AND DRINIA, H., 1993, Architecture and sedimentary facies evolution of a marine, expanding half-graben (Crete, Late Miocene): Basin Research, v. 5, p. 103–124.

PROFFETT, J.M., JR., 1977, Cenozoic geology of the Yerington district, Nevada, and implications for the nature and origin of Basin and Range faulting: Geological Society of America, Bulletin, v. 88, p. 247–266.

RATCLIFFE, N.M., BURTON, W.C., D'ANGELO, R.M., AND COSTAIN, J.K., 1986, Low-angle extensional faulting, reactivated mylonites, and seismic reflection geometry of the Newark Basin margin in eastern Pennsylvania: Geology, v. 14, p. 766–770.

ROBERTS, A., AND YIELDING, G., 1994, Continental extensional tectonics, *in* Hancock, P.L., ed., Continental Deformation: New York, Pergamon, p. 223–250.

ROBSON, D.A., 1971, The structure of the Gulf of Suez (Clysmic) rift, with special reference to the eastern side: Geological Society of London, Journal, v. 127, p. 247–276.

ROSENDAHL, B.R., 1987, Architecture of continental rifts with special reference to East Africa: Annual Review of Earth and Planetary Sciences, v. 15, p. 445–503.

ROSENDAHL, B.R., REYNOLDS, D.J., LORBER, P.M., BURGESS, C.F., McGILL, J., SCOTT, D., LAMBIASE, J.J., AND DERSKEN, S.J., 1986, Structural expressions of rifting: lessons from Lake Tanganyika, Africa, *in* Frostick, L.E., Renault R.W., Reid, I., and Tiercelin, J.–J., eds., Sedimentation in the African Rifts: Geological Society of London, Special Publication 25, p. 29–43.

ROUX, W.F., 1979, The development of growth fault structures: American Association of Petroleum Geologists, Structural Geology Course Notes, 33 p.

RUPPEL, C., 1995, Extensional processes in continental lithosphere: Journal of Geophysical Research, v. 100, p. 24,187–24,215.

SCHLISCHE, R.W., 1990, Aspects of the structural and stratigraphic evolution of early Mesozoic rift basins of eastern North America [unpublished Ph.D. thesis]: Columbia University, New York, 479 p.

SCHLISCHE, R.W., 1991, Half-graben basin filling models: New constraints on continental extensional basin evolution: Basin Research, v. 3, p. 123–141.

SCHLISCHE, R.W., 1992, Structural and stratigraphic development of the Newark extensional basin, eastern North America—implications for the growth of the basin and its bounding structures: Geological Society of America, Bulletin, v. 104, p. 1246–1263.

SCHLISCHE, R.W., 1993, Anatomy and evolution of the Triassic–Jurassic continental rift system, eastern North America: Tectonics, v. 12, p. 1026–1042.

SCHLISCHE, R.W., 1995, Geometry and origin of fault-related folds in extensional settings: American Association of Petroleum Geologists, Bulletin, v. 79, p. 1661–1678.

SCHLISCHE, R.W., AND ANDERS, M.H., 1996, Stratigraphic effects and tectonic implications of the growth of normal faults and extensional basins, *in* Beratan, K.K., ed., Reconstructing the Structural History of Basin and Range Extension Using Sedimentology and Stratigraphy: Geological Society of America, Special Paper 303, p. 183–203.

SCHLISCHE, R.W., AND OLSEN, P.E., 1990, Quantitative filling model for continental extensional basins with applications to early Mesozoic rifts of eastern North America: Journal of Geology, v. 98, p. 135–155.

SCHLISCHE, R.W., YOUNG, S.S., ACKERMANN, R.V., AND GUPTA, A., 1996, Geometry and scaling relations of a population of very small rift-related normal faults: Geology, v. 24, p. 683–686.

SCHLISCHE, R.W., WITHJACK, M.O., AND EISENSTADT, G., 2002, An experimental study of the secondary fault patterns produced by oblique-slip normal faulting: American Association of Petroleum Geologists, Bulletin, v. 86, p. 885–906.

SHARP, I.R., GAWTHORPE, R.L., UNDERHILL, J.R., AND GUPTA, S., 2000, Fault-propagation folding in extensional settings—examples of structural style and synrift sedimentary response from the Suez rift, Sinai, Egypt: Geological Society of America, Bulletin, v. 112, p. 1877–1899.

SITTLER, C., 1969, The sedimentary trough of the Rhine Graben: Tectonophysics, v. 8, p. 543–560.

SMOOT, J.P., 1991, Sedimentary facies and depositional environments of early Mesozoic Newark Supergroup basins, eastern North America: Palaeogeography, Palaeoclimatology, Palaeoecology, v. 84, p. 369–423.

STECKLER, M.S., 1981, The thermal and mechanical evolution of Atlantic-type continental margins [unpublished Ph.D. dissertation]: Columbia University, New York, 261 p.

STECKLER, M.S., 1985, Uplift and extension at the Gulf of Suez: implications of induced mantle convection: Nature, v. 317, p. 135–139.

STEIN, R.S., KING, G.C.P., AND RUNDLE, J.B., 1988, The growth of geological structures by repeated earthquakes; 2. field examples of continental dip-slip faults: Journal of Geophysical Research, v. 93, p. 13,319–13,331.

TANKARD, A.J., AND WELSINK, H.J., 1989, Mesozoic extension and styles of basin formation in Atlantic Canada, in Tankard, A.J., and Balkwill, H.R., eds., Extensional Tectonics and Stratigraphy of the North Atlantic Margins: American Association of Petroleum Geologists, Memoir 46, p. 175–195.

THIEBAUD, C.E., AND ROBSON, D.A., 1979, The geology of the area between Wadi Warden and Wadi Gharandal, east Clysmic rift, Sinai, Egypt: Journal of Petroleum Geology, v. 1, p. 63–75.

THIEBAUD, C.E., AND ROBSON, D.A., 1981, The geology of Asl oilfield, western Sinai, Egypt: Journal of Petroleum Geology, v. 4, p. 77–87.

TRON, V., AND BRUN, J.-P., 1991, Experiments on oblique rifting in brittle–ductile systems: Tectonophysics, v. 188, p. 71–84.

VENDEVILLE, B., 1987, Champs de failles et tectonique en extension: modélisation expérimentale [unpublished Ph.D. dissertation]: Université de Rennes, France, 395 p.

WALSH, J.J., AND WATTERSON, J., 1987, Distributions of cumulative displacement and seismic slip on a single normal fault surface: Journal of Structural Geology, v. 9, p. 1039–1046.

WITHJACK, M.O., AND CALLAWAY, J.S., 2000, Active normal faulting beneath a salt layer—an experimental study of deformation in the cover sequence: American Association of Petroleum Geologists, Bulletin, v. 84, p. 627–651.

WITHJACK, M.O., AND DRICKMAN POLLOCK, D.J., 1984, Synthetic seismic-reflection profiles and rift-related structures: American Association of Petroleum Geologists, Bulletin, v. 68, p. 1160–1178.

WITHJACK, M.O., AND EISENSTADT, G., 1999, Structural history of the Northwest Shelf, Australia—an integrated geological, geophysical and experimental approach (abstract): American Association of Petroleum Geologists, Program and Abstracts, v. 8, p. A151.

WITHJACK, M.O., AND INGEBRIGTSEN, M., 1999, Basement-involved and detached extensional structures—examples from the Norwegian Sea (abstract): American Association of Petroleum Geologists, Program and Abstracts, p. 509.

WITHJACK, M.O., AND JAMISON, W.R., 1986, Deformation produced by oblique rifting: Tectonophysics, v. 126, p. 99–124.

WITHJACK, M.O., AND PETERSON, E., 1993, Prediction of normal-fault geometries—a sensitivity analysis: American Association of Petroleum Geologists, Bulletin, v. 77, p. 1860–1873.

WITHJACK, M.O., MEISLING, K.E., AND RUSSELL, L.R., 1989, Forced folding and basement-detached normal faulting in the Haltenbanken area, offshore Norway, in Tankard, A.J., and Balkwill, H.R., eds., Extensional Tectonics and Stratigraphy of the North Atlantic Margins: American Association of Petroleum Geologists, Memoir 46, p. 567–575.

WITHJACK, M.O., OLSON, J., AND PETERSON, E., 1990, Experimental models of extensional forced folds: American Association of Petroleum Geologists, Bulletin, v. 74, p. 1038–1054.

WITHJACK, M.O., ISLAM, Q., AND LAPOINTE, P., 1995a, Normal faults and their hanging-wall deformation—an experimental study: American Association of Petroleum Geologists, Bulletin, v. 79, p. 1–18.

WITHJACK, M.O., OLSEN, P.E., AND SCHLISCHE, R.W., 1995b, Tectonic evolution of the Fundy basin, Canada: Evidence of extension and shortening during passive-margin development: Tectonics, v. 14, p. 390–405.

WITHJACK, M.O., SCHLISCHE, R.W., AND OLSEN, P.E., 1998, Diachronous rifting, drifting, and inversion on the passive margin of central eastern North America—an analog for other passive margins: American Association of Petroleum Geologists Bulletin, v. 82, p. 817–835.

XIAO, H., AND SUPPE, J., 1992, Origin of rollover: American Association of Petroleum Geologists, Bulletin, v. 76, p. 509–529.

ZANDT, G., AND OWENS, T.J., 1980, Crustal flexure associated with normal faulting and implications for seismicity along the Wasatch front, Utah: Seismological Society of America, Bulletin, v. 70, p. 1501–1520.

ZHANG, P., SLEMMONS, D.B., AND MAO, F., 1991, Geometric pattern, rupture termination and fault segmentation of the Dixie Valley–Pleasant Valley active normal fault system, Nevada, U.S.A.: Journal of Structural Geology, v. 13, p. 165–176.

ZIEGLER, P.A., 1992, European Cenozoic rift system: Tectonophysics, v. 208, p. 91–111.